REFERENCES

Anisman H, Zaharia MD, Meaney MJ, Merali Z. 1998. Do early-life events permanently alter behavioral and hormonal responses to stressors? Int J Dev Neurosci 16:149–164.

Berridge MJ. 1993. Inositol trisphosphate and calcium signalling. Nature 361:315–325.

Bremner JD, Randall P, Scott TM, Bronen RA, Seibyl JP, Southwick SM, Delaney RC, McCarthy G, Charney DS, Innis RB. 1995. MRI-based measurement of hippocampal volume in patients with combat-related posttraumatic stress disorder. Am J Psychiatry 152: 973–981.

Bremner JD, Vythilingam M, Vermetten E, Southwick SM, McGlashan T, Nazeer A, Khan S, Vaccarino LV, Soufer R, Garg PK, Ng CK, Staib LH, Duncan JS, Charney DS. 2003. MRI and PET study of deficits in hippocampal structure and function in women with childhood sexual abuse and posttraumatic stress disorder. Am J Psychiatry 160:924–932.

Francis DD, Diorio J, Plotsky PM, Meaney MJ. 2002. Environmental enrichment reverses the effects of maternal separation on stress reactivity. J Neurosci 22:7840–7843.

Gilmer WS, McKinney WT. 2003. Early experience and depressive disorders: human and non-human primate studies. J Affect Disord 75:97–113.

Gould E, McEwen BS, Tanapat P, Galea LA, Fuchs E. 1997. Neurogenesis in the dentate gyrus of the adult tree shrew is regulated by psychosocial stress and NMDA receptor activation. J Neurosci 17: 2492–2498.

Gould E, Tanapat P, McEwen BS, Flugge G, Fuchs E. 1998. Proliferation of granule cell precursors in the dentate gyrus of adult monkeys is diminished by stress. Proc Natl Acad Sci U S A 95:3168–3171.

Huang LT, Holmes GL, Lai MC, Hung PL, Wang CL, Wang TJ, Yang CH, Liou CW, Yang SN. 2002. Maternal deprivation stress exacerbates cognitive deficits in immature rats with recurrent seizures. Epilepsia 43:1141–1148.

Huot RL, Plotsky PM, Lenox RH, McNamara RK. 2002. Neonatal maternal separation reduces hippocampal mossy fiber density in adult Long Evans rats. Brain Res 950:52–63.

Izumi Y, Zorumski CF. 1999. Norepinephrine promotes long-term potentiation in the adult rat hippocampus in vitro. Synapse 31:196–202.

Kalinichev M, Easterling KW, Plotsky PM, Holtzman SG. 2002. Long-lasting changes in stress-induced corticosterone response and anxiety-like behaviors as a consequence of neonatal maternal separation in Long-Evans rats. Pharmacol Biochem Behav 73:131–140.

Kehoe P, Bronzino JD. 1999. Neonatal stress alters LTP in freely moving male and female adult rats. Hippocampus 9:651–658.

Kehoe P, Clash K, Skipsey K, Shoemaker WJ. 1996a. Brain dopamine response in isolated 10-day-old rats: assessment using D2 binding and dopamine turnover. Pharmacol Biochem Behav 53:41–49.

Kehoe P, Shoemaker WJ, Triano L, Hoffman J, Arons C. 1996b. Repeated isolation in the neonatal rat produces alterations in behavior and ventral striatal dopamine release in the juvenile after amphetamine challenge. Behav Neurosci 110:1435–1444.

Kempermann G, Kuhn HG, Gage FH. 1997. More hippocampal neurons in adult mice living in an enriched environment. Nature 386: 493–495.

Kida S, Josselyn SA, de Ortiz SP, Kogan JH, Chevere I, Masushige S, Silva AJ. 2002. CREB required for the stability of new and reactivated fear memories. Nat Neurosci 5:348–355.

Kitazawa T, Maezono Y, Taneike T. 2000. The mechanisms of alpha (2)-adrenoceptor agonist-induced contraction in longitudinal muscle of the porcine uterus. Eur J Pharmacol 390:185–195.

Kobayashi K, Yasoshima Y. 2001. The central noradrenaline system and memory consolidation. Neuroscientist 7:371–376.

Kobayashi M, Imamura K, Kaub PA, Nakadate K, Watanabe Y. 1999. Developmental regulation of intracellular calcium by N-methyl-D-aspartate and noradrenaline in rat visual cortex. Neuroscience 92:1309–1322.

Kudo Y, Ito K, Miyakawa H, Izumi Y, Ogura A, Kato H. 1987. Cytoplasmic calcium elevation in hippocampal granule cell induced by perforant path stimulation and L-glutamate application. Brain Res 407:168–172.

Liu D, Caldji C, Sharma S, Plotsky PM, Meaney MJ. 2000. Influence of neonatal rearing conditions on stress-induced adrenocorticotropin responses and norepinepherine release in the hypothalamic paraventricular nucleus. J Neuroendocrinol 12:5–12.

MacVicar BA, Tse FW. 1988. Norepinephrine and cyclic adenosine 3':5'-cyclic monophosphate enhance a nifedipine-sensitive calcium current in cultured rat astrocytes. Glia 1:359–365.

Matthews K, Dalley JW, Matthews C, Tsai TH, Robbins TW. 2001. Periodic maternal separation of neonatal rats produces region- and gender-specific effects on biogenic amine content in postmortem adult brain. Synapse 40:1–10.

McCormick CM, Kehoe P, Mallinson K, Cecchi L, Frye CA. 2002. Neonatal isolation alters stress hormone and mesolimbic dopamine release in juvenile rats. Pharmacol Biochem Behav 73:77–85.

Meaney MJ, Diorio J, Francis D, Widdowson J, LaPlante P, Caldji C, Sharma S, Seckl JR, Plotsky PM. 1996. Early environmental regulation of forebrain glucocorticoid receptor gene expression: implications for adrenocortical responses to stress. Dev Neurosci 18:49–72.

Minneman KP. 1988. Alpha 1-adrenergic receptor subtypes, inositol phosphates, and sources of cell Ca2+. Pharmacol Rev 40:87–119.

Minneman KP, Esbenshade TA. 1994. Alpha 1-adrenergic receptor subtypes. Annu Rev Pharmacol Toxicol 34:117–133.

Nakade S, Rhee SK, Hamanaka H, Mikoshiba K. 1994. Cyclic AMP-dependent phosphorylation of an immunoaffinity-purified homotetrameric inositol 1,4,5-trisphosphate receptor (type I) increases Ca2+ flux in reconstituted lipid vesicles. J Biol Chem 269:6735–6742.

Nakano T, Wenner M, Inagaki M, Kugaya A, Akechi T, Matsuoka Y, Sugahara Y, Imoto S, Murakami K, Uchitomi Y. 2002. Relationship between distressing cancer-related recollections and hippocampal volume in cancer survivors. Am J Psychiatry 159:2087–2093.

Nilsson M, Perfilieva E, Johansson U, Orwar O, Eriksson PS. 1999. Enriched environment increases neurogenesis in the adult rat dentate gyrus and improves spatial memory. J Neurobiol 39:569–578.

Okamoto Y, Kagaya A, Motohashi N, Yamawaki S. 1995. Inhibitory effects of lithium ion on intracellular Ca2+ mobilization in the rat hippocampal slices. Neurochem Int 26:233–238.

Pine DS, Cohen JA. 2002. Trauma in children and adolescents: risk and treatment of psychiatric sequelae. Biol Psychiatry 51:519–531.

Plotsky PM, Meaney MJ. 1993. Early, postnatal experience alters hypothalamic corticotropin-releasing factor (CRF) mRNA, median eminence CRF content and stress-induced release in adult rats. Brain Res Mol Brain Res 18:195–200.

Sapolsky RM. 1996. Why stress is bad for your brain. Science 273: 749–750.

Sapolsky RM. 2000. Glucocorticoids and hippocampal atrophy in neuropsychiatric disorders. Arch Gen Psychiatry 57:925–935.

Sapolsky RM, Uno H, Rebert CS, Finch CE. 1990. Hippocampal damage associated with prolonged glucocorticoid exposure in primates. J Neurosci 10:2897–2902.

Silva AJ, Paylor R, Wehner JM, Tonegawa S. 1992a. Impaired spatial learning in alpha-calcium-calmodulin kinase II mutant mice. Science 257:206–211.

Silva AJ, Stevens CF, Tonegawa S, Wang Y. 1992b. Deficient hippocampal long-term potentiation in alpha-calcium-calmodulin kinase II mutant mice. Science 257:201–206.

Uno H, Tarara R, Else JG, Suleman MA, Sapolsky RM. 1989. Hippocampal damage associated with prolonged and fatal stress in primates. J Neurosci 9:1705–1711.

Vythilingam M, Heim C, Newport J, Miller AH, Anderson E, Bronen R, Brummer M, Staib L, Vermetten E, Charney DS, Nemeroff CB, Bremner JD. 2002. Childhood trauma associated with smaller hippocampal volume in women with major depression. Am J Psychiatry 159:2072–2080.

Watanabe Y, Gould E, McEwen BS. 1992. Stress induces atrophy of apical dendrites of hippocampal CA3 pyramidal neurons. Brain Res 588:341–345.

ELSEVIER

Clinical Neuroscience Research 4 (2004) 263–269

Clinical Neuroscience Research

www.elsevier.com/locate/clires

Lithium and protein phosphatases: apoptosis or neurogenesis?

Shigeru Morinobu*, Ki-ichiro Kawano, Shigeto Yamawaki

Division of Frontier Medical Science, Department of Psychiatry and Neurosciences, Programs for Biomedical Research, Graduate School of Biomedical Sciences, Hiroshima University, 1-2-3 Kasumi, Minami-ku, Hiroshima 734-8551, Japan

Abstract

Whereas the effects of lithium on the expression and activity of kinases are extensively examined, relatively little is known about the effect of lithium on the expression and activity of protein phosphatases (PPs). It has been demonstrated that PPs dephosphorylate a number of transcription factors and kinases, leading to decreased gene transcription in the rat brain. Since long-term administration of lithium is required to obtain a therapeutic and prophylactic effect, it is conceivable that regulation of neural plasticity mediated by changes in gene transcription plays an important role in its therapeutic action. In this context, examining the effect of lithium on the expression and activity of PPs may promote our understanding of the molecular action of lithium. In this review, we summarize the results of our studies examining the influence of lithium on the expression and the serine/threonin phosphatase activity of PP2A and 2B, and CREB phosphorylation in the rat brain. We also discuss the putative role of the increased PP2A activity in the therapeutic action of lithium.

Keywords: Apoptosis; Calcineurin; cAMP response element binding protein (CREB); Lithium; Neurogenesis; Protein phosphatase

1. Introduction

An accumulation of evidences derived from clinical studies of mood disorders indicates that long-term administration of mood stabilizers is required to alleviate both manic and depressive features [1,2]. Based on this evidence, it has been postulated that changes in neuronal gene expression induced by repeated, treatments with mood stabilizers, such as lithium or valproate, are involved in the action of these drugs. In this context, there have been numerous preclinical studies examining the effect of chronic administration of mood stabilizers on gene expression [3–7]. For example, Chen and his coworkers [8] demonstrated that long-term treatment with lithium or valproate increased the expression of the antiapoptotic gene, bcl-2, in the rat frontal cortex through an increase in the DNA-binding activity of the transcription factor, polyomavirus enhancer-binding protein 2β. In addition, chronic treatment with these agents led to increased expression of the neuroprotective genes, brain-derived neurotrophic factor (BDNF) and nerve growth factor (NGF) in the rat brain [9,10]. In contrast, expression of the proapoptotic gene, Bax, is decreased in response to long-term administration of lithium [11]. Taken together, the results suggest that several genes involved in neuroprotection are modulated by lithium or valproate, and that the effects upon these genes may be involved in the therapeutic action of these mood stabilizers.

The phosphorylation of transcription factors, such as cAMP response element binding protein (CREB), has also been suggested to play an important role in the therapeutic actions of mood stabilizers [5]. In fact, recent studies have revealed that lithium and valproate regulate the activity of various kinases in the rat brain [6]. For instance, both lithium and valproate have been reported to inhibit the activity of glycogen synthase kinase 3 (GSK-3), and subsequently upregulate gene expression mediated the activation of β-catenin in the rat brain [3,12,13]. Furthermore, lithium and valproate increased the levels of active, phosphorylated extracellular signal-regulated kinase (ERK) 44/42 and active, phosphorylated ribosomal protein S6 kinase-1 in the rat hippocampus and frontal cortex [14]. Yuan and his colleagues [15] demonstrated that long-term administration of lithium increases the levels of phosphorylated c-Jun N-terminal kinases (JNKs) significantly and activates JNK signal transduction. Based on this evidence, it

* Corresponding author. Tel: +81 82 257 5205, fax: +81 82 257 5209.
E-mail address: smoriob@hiroshima-u.ac.jp (S. Morinobu).

1566-2772/$ - see front matter
doi:10.1016/j.cnr.2004.09.003

is conceivable that lithium and valproate regulate gene expression via the activation of several kinases, and that this activity might be associated with the therapeutic action of these mood stabilizers.

In contrast, it has recently been revealed that protein phosphatases dephosphorylate a number of transcription factors and kinases, leading to decreased gene transcription [16,17]. In this context, it is likely that the balance between phosphorylation and dephosphorylation of these factors in the brain regulates neuronal functions via changes in neuronal gene expression. Whereas the influence of mood stabilizers on the activity of protein kinases has been documented [6], relatively little is known of the effect of mood stabilizers on the expression and activity of protein phosphatases in the rat brain [18–20]. The purpose of this review is to summarize the results of our studies examining the influence of mood stabilizers on the expression and the serine/threonin phcsphatase activity of protein phosphatase 2A, 2B (calcineurin), and the expression and phosphorylation state of CREB in the rat brain. Furthermore, we discuss the possible role of mood stabilizers in neuroprotection.

2. Protein phosphatase 2A and lithium

Protein phosphatase 2A (PP2A) has been conserved from yeast to mammals. Protein phosphatase 2A is found as a heterodimer, containing a catalytic subunit C and regulatory subunit A, or as a heterotrimer of subunits A, C, and B. The B subunit has been shown to affect the activity and substrate selectivity of PP2A [16,17,21]. Recent studies have revealed that PP2A plays pivotal roles in the regulation of cell growth, gene expression, and development [17]. For example, the dephosphorylation of CaMK II by PP2A has been reported to influence synaptic strength, as determined by the measurement of long-term depression (LTD) [22]. It has further been suggested that PP2A might regulate gene transcription mediated by the signaling complex of CaMK IV and CREB or of p70 S6 kinase [23,24]. In this context, it is postulated that PP2A may play a fundamental role in gene induction in response to extracellular stimuli.

Recently, the influence of acute and chronic administration of lithium on the expression and the serine/threonin phosphatase activity of PP2A in the rat brain has been extensively examined in our laboratory. To examine the levels of PP2A expression, we performed western blot and immunohistochemical analyses using an anti-goat PP2A C subunit antibody. To examine the level of serine/threonine phosphatase activity of PP2A, the amount of free phosphate derived from the synthetic phosphopeptide RRA(pT)VA (Promega, Madison, WI) was measured by the absorbance of the molybdate-malachite green-phosphate complex using a micro plate reader. Rats were kept on a 0.2% lithium carbonate-containing diet, and normal drinking water and a 1.5% NaCl solution were available to all rats.

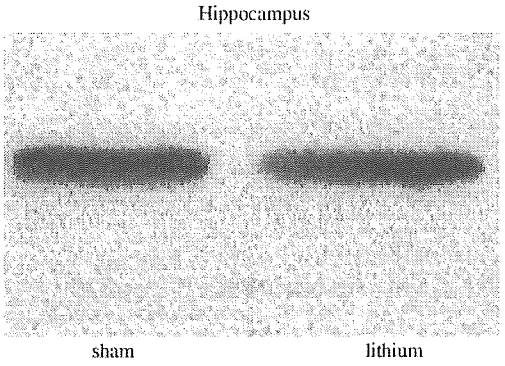

Fig. 1. Western blot analysis of the influence of repeated treatments with lithium (14 d) on PP2A immuoreactivity in the rat hippocampus. Representative immunoblots of the catalytic subunit C of PP2A in the rat hippocampus.

Western blot analyses revealed that the treatment with lithium for either 1 or 14 days had no effect upon the levels of PP2A immunoreactivity in the rat frontal cortex or hippocampus (Fig. 1). Similarly, immunohistochemical analyses demonstrated that administration of lithium for 1 or 14 days had no effect upon PP2A immunoreactivity in either the frontal cortex or hippocampus (Fig. 2).

In contrast, administration of lithium for either 1 or 14 days significantly upregulated the serine/threonine phosphatase activity of PP2A in the rat frontal cortex and hippocampus [20]. Thus, lithium induces the serine/threonine phosphatase activity of PP2A in the rat frontal cortex and hippocampus without affecting its the expression of this enzyme in these regions.

3. Protein phosphatase 2B (calcineurin) and lithium

The Ca^{2+}/calmodulin-dependent protein phosphatase 2B, calcineurin (CaN), is a heterodimer comprising a 61-kDa catalytic subunit (CaN A) and a 19-kDa regulatory subunit (CaN B), that dephosphorylates various substrate proteins [25,26]. The A subunit of CaN is highly expressed in the rat frontal cortex, striatum, and hippocampus [27]. As is the case with PP2A, CaN plays an important role in the synaptic plasticity of hippocampal function, since the sustained phosphorylation of CREB caused by the inhibition of CaN activity promotes the development of LTP [28]. In addition, the dephosphorylation of CREB by the activated inhibitor-1 (I-1) through the dephosphorylation by CaN is, at least in part, involved in the reduction in the rate of gene transcription. In this context, both PP2A and CaN are thought to be involved in the regulation of gene transcription.

Recently, the influence of acute and chronic administration of lithium on the expression and the serine/threonin phosphatase activity of CaN in the rat brain have been extensively examined in our laboratory.

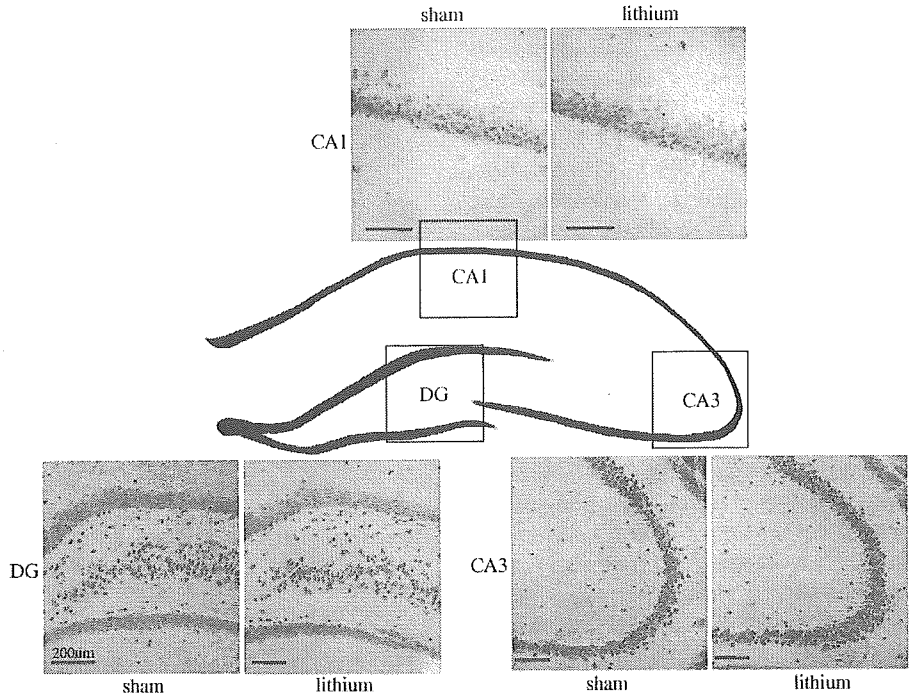

Fig. 2. Immunohistochemical analysis of the influence of repeated treatments with lithium (14 d) on PP2A expression in the rat hippocampus. CA, cornu anmonis; DG, dentate gyrus.

To examine the levels of CaN expression, we performed Northern blot analysis of mRNA expression using a probe from the A subunit of CaN. To examine the level of serine/threonine phosphatase activity of CaN, we used a similar method to that used above for the PP2A study, except that we substituted a different reaction buffer.

Treatment with lithium for either 1 or 14 days had no effect upon the levels of CaN mRNA in the rat frontal cortex and hippocampus (Fig. 3). Similarly, treatment with lithium had no effect upon the serine/threonine phosphatase activity of CaN in these brain regions [18]. Thus, lithium does not affect either the expression or serine/threonine phosphatase activity of CaN in the rat frontal cortex or hippocampus.

4. Protein phosphatases and CREB

It is well known that the phosphorylation of CREB at Ser 133 plays an important role in the transcription of genes, such as c-fos or BDNF, through interaction of the phospho-CREB homodimer with the CRE site located in the promoter region of such genes [29–33]. The activation of several protein kinases, including protein kinase A, calcium/calmodulin-dependent protein kinase II and IV, 90 kDa ribosomal S6 kinase, has been reported to enhance the phosphorylation of CREB [34,35]. On the other hand, various studies have suggested that PPs can downregulate the activity of these protein kinases by their dephosphorylation [16]. For example, the dephosphorylation of I-1 by CaN can increase PP1 activity and subsequently lead to increased dephosphorylation of CREB [36,37]. CaMK II and IV are also dephosphorylated by PP2A through an increase in the intracellular Ca^{2+} concentration, leading to a suppression in the rate of CREB phosphorylation [23,38].

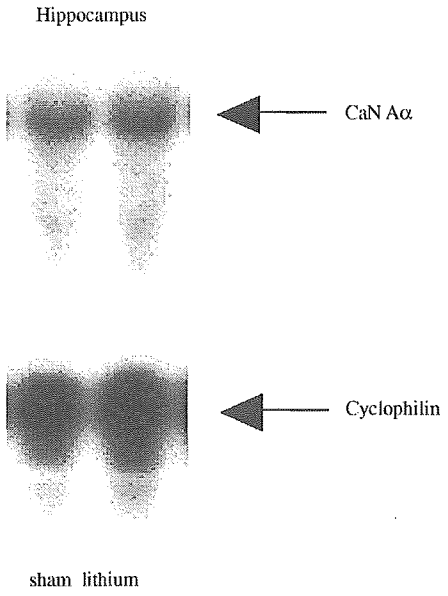

Fig. 3. Northern blot analysis of the influence of repeated treatments with lithium (14 d) on the levels of PP2B mRNA in the rat hippocampus. Representative Northern blot of the subunit A mRNA of PP2B and cyclophilin mRNA in the rat hippocampus.

Various extracellular stimuli, such as neurotrophic factors, result in the activation of the mitogen-activated protein kinase (MAPK)—extracellular signal-regulated kinase (Erk)—90 kDa ribosomal S6 kinase (Rsk) cascade, which also increases the levels of phospho-CREB [5]. In contrast to the phosphorylation of CREB by the MAPK-Erk-Rsk cascade, PP2A has been reported to dephosphorylate protein kinases at several points in this cascade and consequently downregulate the phosphorylation of CREB [16]. In this context, it is conceivable that PPs are involved in the regulation of CRE-mediated gene expression.

5. Lithium and CREB phosphorylation

As described above, the influence of lithium on the phosphorylation state of CREB, which is in turn regulated by the balance between the activity of protein kinases and phosphatases, is thought to be an important component of its mechanism of therapeutic action via its effects upon gene expression. In this context, we performed Western blot analysis to examine whether long-term administration of lithium resulted in changes in the steady-state level of phosphorylated CREB in the rat brain. Western blot analysis revealed a phospho-CREB immunoreactive band of approximately 43 kDa (Fig. 4A). Administration of lithium for 14 days had no effect on the level of phospho-CREB immunoreactivity in the rat frontal cortex or hippocampus

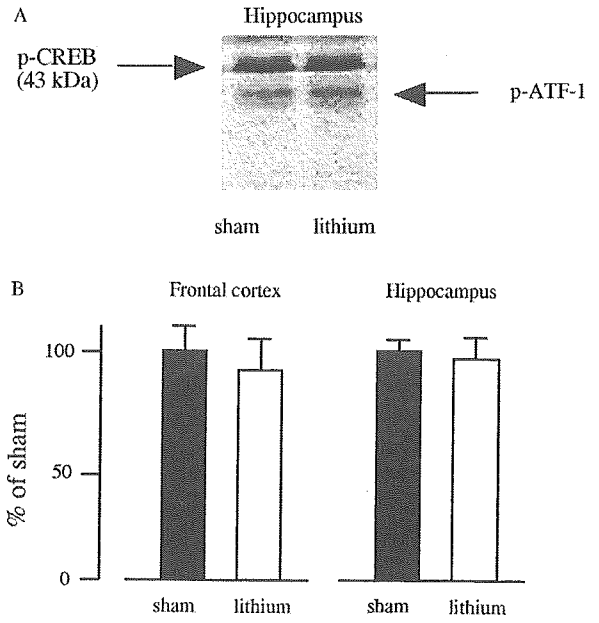

Fig. 4. Western blot analysis of the influence of repeated treatments with lithium (14 d) on the levels of phospho-CREB immunoreactivity in the rat hippocampus. (A) Representative immunoblots of phospho-CREB in the rat hippocampus. (B) Quantification of phospho-CREB immunoreactivity in response to repeated treatments with lithium. Data are presented as percentage of sham-treated rats and are the mean ± SEM of six rats for each treatment group.

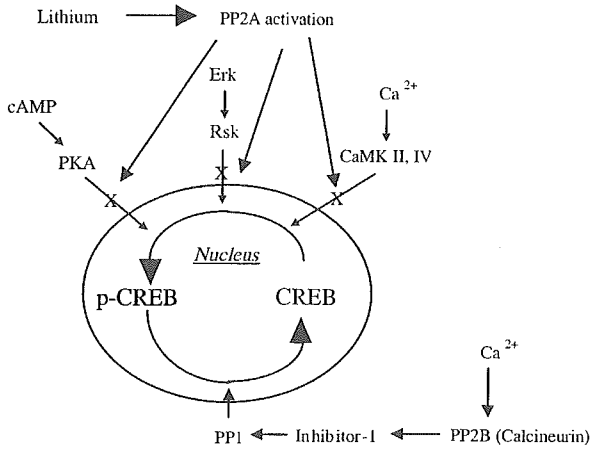

Fig. 5. Regulation of CREB phosphorylation and dephosphorylation by lithium treatment through the balance between the activity of protein kinases and phosphtases. CaM K; calcium/calmodulin-dependent protein kinase, CREB; cAMP response element binding protein, ERK; extracellular signal-regulated kinase, PKA; protein kinase A, PP; protein phosphatase, Rsk; 90 kDa ribosomal S6 kinase.

(Fig. 4B). Thus, repeated treatment with lithium does not affect the phosphorylation of CREB in the rat brain [39].

Although several studies have examined the effect of lithium on the phosphorylation state of CREB, the results are still inconclusive. Chuang and his colleagues demonstrated that chronic lithium treatment enhanced the phosphorylation of CREB in cultures of cerebellar granular neurons and human neuroblastoma SH-SY5Y cells [19,40]. Similary, Grimes and Jope demonstrated that lithium increased the DNA binding activity of CREB in human neuroblastoma SSH-SY5Y cells. Conversely, Young and his coworkers demonstrated that chronic lithium treatment decreased CREB phosphorylation in cultures of human neuroblastoma SH-SY5Y cells and in the rat brain [41,42]. Our results are inconsistent with these previous findings. Since various signal transduction pathways involving numerous protein kinases and phosphatases are involved in the phosphorylation of CREB, it is likely that different experimental procedures may lead to the discordant effects of lithium on CREB phosphorylation. We speculate that the effect of lithium on the activity of kinases may have been counteracted by its effects on the activity of phosphatases under the experimental conditions we used. Thus, no significant change in the steady-state level of phosphorylation of CREB was found in response to long-term lithium administration.

Based on the influence of lithium on the activity of PPs, we summarize the plausible action of lithium on the regulation of CREB phosphorylation (Fig. 5).

6. Lithium and apoptosis

It has been postulated that protein phosphatases play key roles in apoptosis [43,44]. In Fig. 6, we propose mechanisms

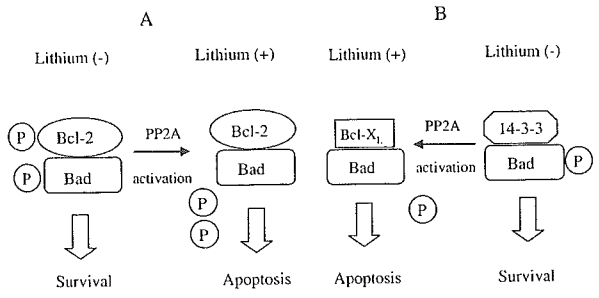

Fig. 6. Regulation of apoptotic signal transductions by lithium treatment through Bcl-2 (A) (modified from Garcia et al.), and Bad (B) (modified from Klumpp and Krieglstein).

by which PP1, PP2A, and PP2B induce apoptosis. Growing evidence suggests that the dephosphorylation of the anti-apoptotic protein, Bcl-2, plays an important role in the induction of apoptosis [45,46]. In particular, Ruvolo et al. [47] demonstrate that the rapid Bcl-2 dephosphorylation in response to ceramide induces apoptosis and that the activation of mitochondrial PP2A, which is colocalized with Bcl-2 at the mitochindrial membrane, is closely involved in this ceramide-induced apoptosis. In addition to Bcl-2, PP1, PP2A, and PP2B are responsible for the dephosphorylation of the proapoptotic protein, BAD [48–50]. It has been reported that phosphorylated BAD located at the mitochondrial surface can bind to cytoplasmic 14-3-3 proteins, which in turn leads to the inhibition of the apoptotic activity of BAD [51]. On the other hand, dephosphorylated BAD, arising from the action of protein phosphatases, can bind to Bcl-XL and subsequently inhibit its antiapoptotic activity [44]. In this context, our finding that lithium administration increases the activity of PP2A in the rat brain suggests that it may result in the enhancement of the apoptotic activity mediated by BAD, due to enhanced dephosphorylation of BAD under these conditions.

The results of our studies indicate that administration of lithium for either 1 or 14 days significantly upregulates the activity of PP2A, but not PP2B [18,22]. These data suggest that lithium has an apoptotic action in the central nervous system. This finding contrasts with previous evidence indicating that lithium has potent neuroprotective effects.

However, it remains plausible that lithium may have an apoptotic effect. It is well known that long-term lithium administration is required to obtain a therapeutic and prophylaxic effect in the treatment of bipolar mood disorder. If long-lasting neuroprotective and neurotprophic effects, such as neurogenesis, are continually induced during lithium treatment, neuronal hyperplasia may result. However, there is no evidence that long-term administration of lithium increases the prevalence of hyperplastic change in the central nervous system, although chronic lithium treatment (4 w) is reported to increase the grey matter volume in patients with bipolar disorder [52]. In contrast, it is well known that lithium treatment induces parathyroid hyperplasia and epidermal hyperplasia [53–58]. In this context, apoptotic effects induced by the activation of PP2A in response to lithium might play an important role in the control of various cellular processes, such as degradation and regeneration.

7. Conclusion

Numerous studies have postulated that potent neurotrophic and neuroprotective effects are an important component of the therapeutic action of chronic lithium treatment. Changes in neuronal gene expression resulting from the activation of various protein kinases may represent one means by which lithium exerts its therapeutic action. However, the regulation of protein phosphorylation by protein kinases and phosphatases plays an important role in the morphogenesis of neurons and glia cells. In this context, it is likely that the activation of protein phosphatases by lithium may regulate the neurogenetic action of lithium. Further studies examining the influence of lithium on apoptosis and neurogenesis in protein phosphatase knock-down animals using double-stranded RNA-mediated RNA interference should help us elucidate the role of protein phosphatases in the therapeutic action of this mood-stabilizing agent.

Acknowledgements

This study was supported by a grant-in-aid for general scientific research from the Ministry of Education, Science, and Culture of Japan, a Health Science Research Grant for Research on Brain Science from the Ministry of Health and Welfare of Japan, a grant from Core Research for Evolutional Science and Technology (CREST) and a grant from Target Oriented Brain Science Promotion Program supported by the MEXT of Japan Science and Technology (JST).

References

[1] Goodwin PK, Jamison KR. Manic-depressive illness. New York, NY: Oxford University; 1990.
[2] Jefferson JW, Greist KD. Lithium. In: Kaplan HI, Sadock BJ, editors. Comprehensive textbook of psychiatry. Baltimore: Williams & Wilkins; 1995. p. 2022–30.
[3] Ikonomov OC, Manji HK. Molecular mechanisms underlying mood stabilization in manic-depressive illness: the phenotype challenge. Am J Psychiatry 1999;156(10):1506–14.
[4] Manji HK, Moore GJ, Rajkowska G, Chen G. Neuroplasticity and cellular resilience in mood disorders. Mol Psychiatry 2000;5(6): 578–93.
[5] Duman RS. Synaptic plasticity and mood disorders. Mol Psychiatry 2002;7(1):S29–S34.
[6] Manji HK, Chen G. PKC MAP Kinases and the bcl-2 family of proteins as long-term targets for mood stabilizers. Mol Psychiatry 2002;7(1):S46–S56.

[7] Lenox RH, Wang L. Molecular basis of lithium action: integration of lithium-responsive signaling and gene expression networks. Mol Psychiatry 2003;8(2):135–44.
[8] Chen G, Zeng WZ, Yuan PX, Huang LD, Zeng WZ, Yuan PX, et al. The mood-stabilizing agents lithium and valproate robustly increase the lev els of the neuroprotective protein bcl-2 in the CNS. J Neurochem 1999;72(2):879–82.
[9] Hellweg R, Lang UE, Nagel M, Baumgartner A. Subchronic treatment with lithium increases nerve growth factor content in distinct brain regions of adult rats. Mol Psychiatry 2002;7(6):604–8.
[10] Fukumoto T, Morinobu S, Okamoto Y, Kagaya A, Yamawaki S. Chronic lithium treatment increases the expression of brain-derived neurotrophic factor in the rat brain. Psychopharmacology (Berl) 2001; 158(1):100–6.
[11] Chen RW, Chuang DM. Long term lithium treatment suppresses p53 and Bax expression but increases Bcl-2 expression. A prominent role in neuroprotection against excitotoxicity. J Biol Chem 1999;274(10): 6039–42.
[12] Chen G, Huang LD, Jiang YM, Manji HK. The mood-stabilizing agent valproate inhibits the activity of glycogen synthase kinase-3. J Neurochem 1999;72(3):1327–30.
[13] Jope RS. Anti-bipolar therapy: mechanism of action of lithium. Mol Psychiatry 1999;4(2):117–28.
[14] Yuan PX, Huang LD, Jiang YM, Gutkind JS, Manji HK, Chen G. The mood stabilizer valproic acid activates mitogen-activated protein kinases and promotes neurite growth. J Biol Chem 2001;276(34): 31674–83 [Epub 2001 Jun 19].
[15] Yuan P, Chen G, Manji HK. Lithium activates the c-Jun NH2-terminal kinases in vitro and in the CNS in vivo. J Neurochem 1999; 73(6):2299–309.
[16] Millward TA, Zolnierowicz S, Hemmings BA. Regulation of protein kinase cascades by protein phosphatase 2A. Trends Biochem Sci 1999;24(5):1 see also pages 86–91.
[17] Goldberg Y. Protein phosphatase 2A: who shall regulate the regulator? Biochem Pharmacol 1999;57(4):321–8.
[18] Tanaka K, Takahashi J, Morinobu S, Koichieo F, Seiichi T, Kunio K, et al. Imipramine, but not lithium, induces the serine/threonine phosphatase activity of calcineurin without affecting its mRNA expression in the rat brain. Psychopharmacology (Berl) 2002;162(3): 339–44.
[19] Kopnisky KL, Chalecka-Franaszek E, Gonzalez-Zulueta M, Chuang DM. Chronic lithium treatment antagonizes glutamate-induced decrease of phosphorylated CREB in neurons via reducing protein phosphatase 1 and increasing MEK activities. Neuroscience 2003;116(2):425–35.
[20] Tsuji S, Morinobu S, Tanaka K, Kawano K, Yamawaki S. Lithium, but not valproate, induces the serine/threonine phosphatase activity of protein phosphatase 2A in the rat brain, without affecting its expression. J Neural Trans 2003;110(4):413–25.
[21] Garcia A, Cayla X, Sontag E. Protein phosphatase 2A: a definite player in viral and parasitic regulation. Microbes Infect 2000;2(4): 401–7.
[22] Mulkey RM, Herron CE, Malenka RC. An essential role for protein phosphatases in hippocampal long-term depression. Science 1993; 261(5124):1051–5.
[23] Westphal RS, Anderson KA, Means AR, Wadzinski BE. A signaling complex of Ca^{2+}-calmodulin-dependent protein kinase IV and protein phosphatase 2A. Science 1998;280(5367):1258–61.
[24] Westphal RS, Coffee Jr RL, Marotta A, Pelech SL, Wadzinski BE. Identification of kinase-phosphatase signaling modules composed of p70 S6 kinase-protein phosphatase 2A (PP2A) and p21-activated kinase-PP2A. J Biol Chem 1999;274(2):687–92.
[25] Klee CB, Crouch TH, Krinks MH. Calcineurin: a calcium- and calmodulin-binding protein of the nervous system. Proc Natl Acad Sci USA 1979;76(12):6270–3.
[26] Cohen P. The structure and regulation of protein phosphatases. Annu Rev Biochem 1989;58:453–508.
[27] Kuno T, Mukai H, Ito A, Chang CD, Kishima K, Saito N, Tanaka C, et al. Distinct cellular expression of calcineurin A alpha and A beta in rat brain. J Neurochem 1992;58(5):1643–51.
[28] Bito H, Deisseroth K, Tsien RW. CREB phosphorylation and dephosphorylation: a Ca(2+)- and stimulus duration-dependent switch for hippocampal gene expression. Cell 1996;87(7): 1203–14.
[29] Gonzalez GA, Montminy MR. Cyclic AMP stimulates somatostatin gene transcription by phosphorylation of CREB at serine 133. Cell 1989;59(4):675–80.
[30] Sheng M, McFadden G, Greenberg ME. Membrane depolarization and calcium induce c-fos transcription via phosphorylation of transcription factor CREB. Neuron 1990;4(4):571–82.
[31] Brindle PK, Montminy MR. The CREB family of transcription activators. Curr Opin Genet Dev 1992;2(2):199–204.
[32] Shieh PB, Hu SC, Bobb K, Timmusk T, Ghosh A. Identification of a signaling pathway involved in calcium regulation of BDNF expression. Neuron 1998;20(4):727–40.
[33] Tao X, Finkbeiner S, Arnold DB, Shaywitz AJ, Greenberg ME. Ca^{2+} influx regulates BDNF transcription by a CREB family transcription factor-dependent mechanism. Neuron 1998;20(4):709–26.
[34] Matthews RP, Guthrie CR, Wailes LM, Zhao X, Means AR, McKnight GS. Calcium/calmodulin-dependent protein kinase types II and IV differentially regulate CREB-dependent gene expression. Mol Cell Biol 1994;14(9):6107–16.
[35] Dash PK, Karl KA, Colicos MA, Prywes R, Kandel ER. cAMP response element-binding protein is activated by Ca^{2+}/calmodulin-as well as cAMP-dependent protein kinase. Proc Natl Acad Sci USA 1991;88(11):5061–5.
[36] Winder DG, Mansuy IM, Osman M, Moallem TM, Kandel ER. Genetic and pharmacological evidence for a novel, intermediate phase of long-term potentiation suppressed by calcineurin. Cell 1998;92(1): 25–37.
[37] Mulkey RM, Endo S, Shenolikar S, Malenka RC. Involvement of a calcineurin/inhibitor-1 phosphatase cascade in hippocampal long-term depress ion. Nature 1994;369(6480):486–8.
[38] Barnes GN, Slevin JT, Vanaman TC. Rat brain protein phosphatase 2A: an enzyme that may regulate autophosphorylated protein kinases. J Neurochem 1995;64(1):340–53.
[39] Morinobu S, Yamawaki S, Fukumoto T, Tsuji S, Suenaga T, Takahashi J, Tanaka T, Fujimaki K. Lithium and signal transduction. In: Nagatsu T, editor. Catecholamine research: from molecular insights to clinical medicine. New York: Academic Plenum Publishers; 2002. p. 435–7.
[40] Ozaki N, Chuang DM. Lithium increases transcription factor binding to AP-1 and cyclic AMP-responsive element in cultured neurons and rat brain. J Neurochem 1997;69(6):2336–44.
[41] Chen B, Wang JF, Hill BC, Young LT. Lithium and valproate differentially regulate brain regional expression of phosphorylated CREB and c-Fos. Brain Res Mol Brain Res 1999;70(1):45–53.
[42] Wang JF, Asghari V, Rockel C, Young LT, Cyclic AMP. responsive element binding protein phosphorylation and DNA binding is decreased by chronic lithium but not valproate treatment of SH-SY5Y neuroblastoma cells. Neuroscience 1999;91(2):771–6.
[43] Garcia A, Cayla X, Guergnon J, Dessauge F, Hospital V, PAZ Rebollom M, et al. Serine/threonine protein phosphatases PP1 and PP2A are key players in apoptosis. Biochimie 2003;85(8):721–6.
[44] Klumpp S, Krieglstein J. Serine/threonine protein phosphatases in apoptosis. Curr Opin Pharmacol 2002;2(4):458–62.
[45] Ruvolo PP, Deng X, Carr BK, May WS. A functional role for mitochondrial protein kinase Calpha in Bcl2 phosphorylation and suppression of apoptosis. J Biol Chem 1998;273(39):25436–42.
[46] Deng X, Ito T, Carr B, Mumby M, May Jr WS. Reversible phosphorylation of Bcl2 following interleukin 3 or bryostatin 1 is mediated by direct interaction with protein phosphatase 2A. J Biol Chem 1998;273(51):34157–63.

[47] Ruvolo PP, Deng X, Ito T, Carr BK, May WS. Ceramide induces Bcl2 dephosphorylation via a mechanism involving mitochondrial PP2A. J Biol Chem 1999;274(29):20296–300.

[48] Wang HG, Pathan N, Ethell IM, et al. Ca^{2+}-induced apoptosis through calcineurin dephosphorylation of BAD. Science 1999; 284(5412):339–43.

[49] Ayllon V, Martinez AC, Garcia A, Cayla X, Rebollo A. Protein phosphatase 1alpha is a Ras-activated Bad phosphatase that regulates interleukin-2 deprivation-induced apoptosis. Eur. Mol. Biol. Org. J. 2000;19(10):2237–46.

[50] Chiang CW, Harris G, Ellig C, et al. Protein phosphatase 2A activates the proapoptotic function of BAD in interleukin-3-dependent lymphoid cells by a mechanism requiring 14-3-3 dissociation. Blood 2001;97(5):1289–97.

[51] Zha J, Harada H, Osipov K, Jockel J, Waksman G, Korsmeyer SJ. BH3 domain of BAD is required for heterodimerization with BCL-XL and pro-apoptotic activity. J Biol Chem 1997;272(39):24101–4.

[52] Moore GJ, Bebchuk JM, Wilds IB, Chen G, Manji HK, Menji HK. Lithium-induced increase in human brain grey matter. Lancet 2000; 356(9237):1241–2.

[53] Mallette LE, Khouri K, Zengotita H, Hollis BW, Malini S. Lithium treatment increases intact and midregion parathyroid hormone and parathyroid volume. J Clin Endocrinol Metab 1989;68(3):654–60.

[54] Stancer HC, Forbath N. Hyperparathyroidism, hypothyroidism, and impaired renal function after 10 to 20 years of lithium treatment. Arch Intern Med 1989;149(5):1042–5.

[55] Saxe AW, Gibson G. Lithium increases tritiated thymidine uptake by abnormal human parathyroid t issue. Surgery 1991;110(6):1067–76 [discussion 1076–7].

[56] Nordenstrom J, Strigard K, Perbeck L, Willems J, Bagedahl-Strindlund M, Linder J. Hyperparathyroidism associated with treatment of manic-depressive disorders by lithium. Eur J Surg 1992;158(4):207–11.

[57] Wolf R, D'Avino M, De Angelis F, et al. Effects of lithium carbonate (Li2CO3) on in-vitro-cultured normal human skin explants Correlation of serum interleukin-8 and cell surface lysosome-associated membrane protein expression with clinical disease activity in systemic lupus erythematosus Granted publications: taken for granted? J Eur Acad Dermatol Venereol 2000;14(2):97–9.

[58] Awad SS, Miskulin J, Thompson N. Parathyroid adenomas versus fourgland hyperplasia as the cause of primary hyperparathyroidism in patients with prolonged lithium therapy. World J Surg 2003;27(4): 486–8.

Brain activity during expectancy of emotional stimuli: an fMRI study

Kazutaka Ueda,[1,2] Yasumasa Okamoto,[1] Go Okada,[1] Hidehisa Yamashita,[1] Tadao Hori[2] and Shigeto Yamawaki[1,CA]

[1]Department of Psychiatry and Neurosciences, Division of Frontier Medical Science, Programs for Biomedical Research, Graduate School of Biomedical Sciences, Hiroshima University, 1-2-3, Kasumi, Minami-ku, Hiroshima 734-8551; [2]Department of Behavioral Sciences, Faculty of Integrated Arts and Sciences, Hiroshima University, 1-7-1, Kagamiyama, Higashi-Hiroshima, Hiroshima 739-8521, Japan

[CA]Corresponding Author

Received 30 October 2002; accepted 18 November 2002

DOI: 10.1097/01.wnr.0000050712.17082.1c

We studied the neural activation associated with the expectancy of emotional stimuli using whole brain fMRI. Fifteen healthy subjects underwent fMRI scanning during which they performed a warned reaction task using emotional pictures carrying pleasant, unpleasant, or neutral content. The task involved an expected or unexpected condition. Data were analyzed by comparing the images acquired under the different conditions. In the expected condition, compared with the unexpected condition, significant activation was observed in the medial, inferior and dorsolateral prefrontal cortex. Whereas the expectancy of pleasant stimuli produced activation in the left dorsolateral and left medial prefrontal cortex as well as in the right cerebellum, the expectancy of unpleasant stimuli produced activation in the right inferior and right medial prefrontal cortex, the right amygdala, the left anterior cingulate cortex, and bilaterally in the visual cortex. These results suggest that the expectancy of emotional stimuli is mediated by the prefrontal area including the medial, inferior, and dorsolateral prefrontal cortex. Furthermore, our data suggest that left frontal activation is associated with the expectancy of pleasant stimuli and that right frontal activation is associated with the expectancy of unpleasant stimuli. Finally, our findings suggest that the amygdala and anterior cingulate cortex may play an important role in the expectancy of unpleasant stimuli and that the input of this negative information is modulated by these specific brain areas. *NeuroReport* 14:51–55 © 2003 Lippincott Williams & Wilkins.

Key words: Amygdala; Anterior cingulate cortex; Expectancy; Emotion; fMRI; Prefrontal cortex

INTRODUCTION

Emotional responses are thought to play a vital role in survival and in our ability to adapt to our environment [1,2]. It has been suggested that the mechanism by which we process emotional information consists of evaluative, experiential, and expressive components [3]. Evaluation in the present of emotional events that are destined to happen in the future is a necessary form of adaptive behavior.

Recent functional neuroimaging studies have suggested that the amygdala [4–8], anterior cingulate cortex (ACC) [6,9–11] and occipital cortex [7,12] respond to unpleasant stimuli, and that the ACC [10], the medial and orbital, as well as the dorsolateral prefrontal cortex (PFC) [7] and the occipital cortex [7,12] respond to pleasant stimuli. However, little is known about brain activity during the expectancy of emotional stimuli. In this study, we set out to determine which brain regions were associated with the expectancy of emotional stimuli in humans. Brain activation was measured in healthy subjects with fMRI using blood oxygen level dependent (BOLD) contrast while the subjects performed a warned reaction task using pictures which evoked emotionally pleasant, unpleasant, or neutral content.

MATERIALS AND METHODS

Fifteen, right-handed healthy volunteers (seven men and eight women), aged 20–33 years (mean 25 years), with no history of neurological or psychiatric illness, participated in this study. The study was conducted under a protocol that was approved by the Ethics Committee of Hiroshima University School of Medicine. All subjects submitted informed written consent prior to their participation in this study.

Participants were subjected to a warned reaction task. Each trial involved the consecutive presentation of a warning stimulus (geometrical pattern, duration 100 ms) followed 3900 ms later by an emotional picture (duration 2000 ms). Each warning stimulus was presented with a stimulus onset asynchrony of 12 s. Sixty-four digitized color pictures were chosen for use in this study from the International Affective Picture System on the basis of their normative valence ratings (22 pleasant, 22 unpleasant, and 20 neutral) [13]. Subjects were required to respond quickly by pressing a button with their right index finger when they detected an emotional picture. The subjects were administered two alternating experimental conditions. In the

'expected' condition, subjects could anticipate the valence of the emotional picture as a result of seeing the warning stimulus, because the geometrical pattern and the valence category of the emotional picture were fixed (e.g., a circle, pleasant; a triangle, neutral; a square, unpleasant). Combinations were counterbalanced across subjects. In the 'unexpected' condition, the warning stimulus consisted of a cross pattern. In this condition, subjects could not anticipate the valence of the emotional picture as a result of having been shown the warning stimulus. This is the control condition for visuomotor activity. The task consisted of 16 blocks, each of which were preceded by an instruction slide informing the subject as to whether the condition was expected or unexpected. Of these 16 blocks, eight were expected condition and eight were unexpected. Pleasant, unpleasant, and neutral pictures were randomly ordered within each block. The duration of each block was 48 s.

fMRI was performed using a Magnex Eclipse 1.5 T Power Drive 250 (Shimazu Medical Systems, Kyoto, Japan). A time-course series of 227 volumes was acquired with T2*-weighted, gradient echo, echo planar imaging (EPI) sequences. Each volume consisted of 38 slices, with a slice thickness of 4 mm with no gap, and covered the entire cerebral and cerebellar cortices. The interval between two successive acquisitions of the same image (TR) was 4000 ms, the echo time (TE) was 55 ms, and the flip angle was 90°. The field of view (FOV) was 256 mm, and the matrix size was 64 × 64, giving voxel dimensions of 4 × 4 × 4 mm. Scan acquisition was synchronized to the onset of the trial. After functional scanning, structural scans were acquired using a Tl-weighted gradient echo pulse sequence (TR = 12 ms; TE = 4.5 ms; flip angle = 20°; FOV = 256 mm; voxel dimensions of 1 × 1 × 1 mm), which facilitated localization.

Image processing and statistical analyses were carried out using Statistical Parametric Mapping (SPM 99) software (Wellcome Department of Cognitive Neurology, London, UK). The first three volumes of the fMRI run were discarded because the MR signal was unsteady. All EPI images were spatially normalized with the Montreal Neurological Institute (MNI) T1 template for group analysis. Imaging data were corrected for motion and smoothed with an 8 mm full-width, half-maximum Gaussian filter. Using group analysis according to a random effect model, we identified regions that showed significant responses during the expected condition, compared to the unexpected condition. We also employed event-related analysis. We identified regions that showed significant activation during the 4 s delay period (between the presentation of the warning stimulus and the emotional picture) of each category of emotional picture in the expected condition compared to the 4 s delay period in the unexpected condition. Activations were reported if they exceeded $p < 0.001$ (uncorrected) on the single voxel level and $p < 0.05$ (corrected) on the cluster level. The BOLD signal for the pre- and post-warning stimulus were extracted from the clusters in which there was significant activation during the expected condition and averaged. The averaged data were assembled into 16 s time courses.

The xyz coordinates provided by SPM99, which are in MNI brain space, were converted to xyz coordinates in Talairach and Tournoux's brain space [14]. Labels for brain activation foci were obtained in Talairach coordinates using the Talairach Deamon software, which provides state of the art accuracy [15]. The areas identified as labeled areas by this software were then confirmed by comparison with activation maps overlaid on MNI-normalized structural MRI images.

It is possible that differences in the delay period (pleasant, unpleasant, and neutral) could systematically influence a subject's movement in the scanner and contribute to differences in brain activity. To address this issue, we evaluated the translational (x, y, and z) and rotational (pitch, roll, and yaw) movements using ANOVA (valence: pleasant, unpleasant, and neutral). Scan-to-scan movement did not differ in either dimension as a function of valence, indicating that movement did not systematically differ as a function of experimental manipulation and thus did not likely contribute to the observed differences in signal intensity.

RESULTS AND DISCUSSION

The expected condition resulted in a significant activation of the right superior frontal gyrus (Brodmann area (BA) 8), left inferior frontal gyrus (BA 45), and left middle frontal gyrus (BA 6 and 9), compared to the unexpected condition (Fig. 1). No significant activation was detected during the unexpected condition compared to the expected condition.

The delay period of the pleasant picture in the expected condition resulted in significant activation of the left middle frontal gyrus (BA 9), right cerebellum, and left superior frontal gyrus (BA 6; Table 1, Fig. 2a,b). During the delay period of the neutral picture in the expected condition, significant signal increases occurred in the left superior parietal lobule (BA 7), left middle frontal gyrus (BA 46), and left inferior frontal gyrus (BA 44; Table 1). The delay period of the unpleasant picture in the expected condition resulted in significant increases in the right inferior frontal gyrus (BA 47), right amygdala, left anterior cingulate (BA 32), and right medial frontal gyrus (BA 10; Table 1, Fig. 2c,d,e). The bilateral middle occipital gyrus (BA 19), right cuneus (BA 17), and left lingual gyrus (BA 17) were also activated. The BOLD signals within the clusters in which there was significant activation during the expected condition were already elevated before exposure of the subject to the emotional picture (Fig. 2f,g, pleasant, unpleasant, respectively). Therefore, the observed activations were likely to have been expectation-related.

The present study examined human brain activity during a warned reaction task using emotional pictures carrying pleasant, unpleasant, or neutral content. The results may reflect the expectancy of emotional stimuli by the human brain. Results from the present study suggested that the expectancy of emotional stimuli was mediated significantly by the prefrontal area, including the medial, inferior, and dorsolateral PFC. These results are consistent with previously reported findings that suggested that these areas played an important role in emotional cognitive processes [7,8,16–18].

Our data also revealed that a prominent increase in activation of the left dorsolateral and left medial PFC and right cerebellum was associated with the expectancy of a pleasant picture, and that activation of the right inferior and right medial PFC, right amygdala, left ACC, and bilateral

visual cortex was associated with the expectancy of an unpleasant picture. Our finding of an asymmetric hemispheric pattern of activation of the PFC is in concert with findings from published neuropsychological studies. Processing of positive connotations of incoming information was reported to have been accompanied by increased left-sided frontal activation, while processing of negative connotations was accompanied by increased right-sided frontal activation [19,20]. Our data were also consistent with previous research in clinical depression. Patients with depression, a condition that affects the ability to detect and take pleasure in future events, were found to show specific decreases in glucose metabolic activity in their left dorsolateral prefrontal regions [21]. This pattern of decreased activation in the left dorsolateral frontal cortex in depressed individuals may reflect a pervasive deficit in their ability to evaluate emotional events that will happen in the future.

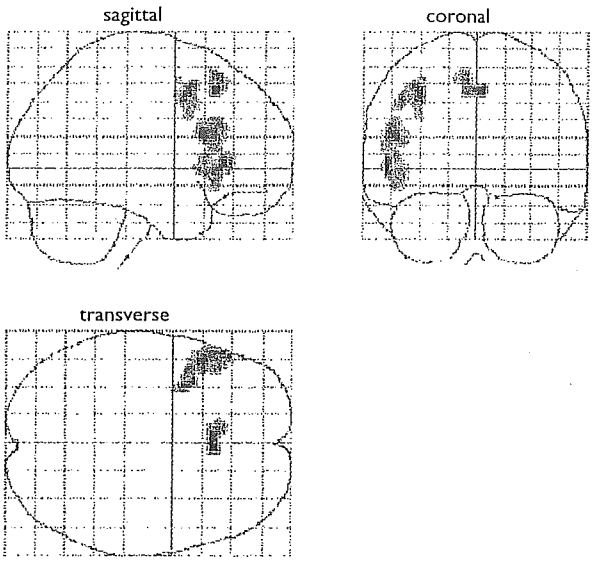

Fig. 1. Statistical parametric maps of brain regions (in the second level group analysis for the 15 subjects) showing significant increases in BOLD contrast associated with the expected condition compared to the unexpected condition at a statistical threshold of $p < 0.001$ (uncorrected) at the single voxel level and $p < 0.05$ (corrected) at the cluster level. Clusters of activation were shown as through-projections onto representations of standard stereotactic space (Sagittal, side view; coronal, view from back; transverse, view from above).

In this study, only the expectancy of an unpleasant picture produced activity in the amygdala and ACC. This finding supports the suggestion that the amygdala plays a vital role in the evaluation of the emotional significance of stimuli [4–8]. Moreover, animal studies have suggested that the amygdala was involved in the evaluation of cues that predict danger to the organism [22]. Our results may extend these observations to humans by showing that the expectancy of unpleasant stimuli was also a function of the amygdala, which thus may play a broader role in coordinating a person's response to an upcoming danger. Anatomical tracing studies suggested that the ACC was subdivided into a rostral-ventral affective division and a dorsal cognitive division, based on their distinct efferent and afferent projection systems [9,23]. Activation observed in this study occurred within the affective division of the ACC. The affective division of the ACC has extensive connections with limbic and paralimbic regions, such as the amygdala and orbitofrontal cortex [9,23], and is primarily involved in assessing the salience of emotional information and in the regulation of the emotional response [9,11,23]. In contrast to our study, Lane *et al.* [10] reported ACC activation in response to both pleasant and unpleasant pictures as opposed to just in response to unpleasant pictures. The discrepancy between their findings and ours may have been due to task differences. While Lane and colleagues [10] examined neural activity during the viewing of emotional pictures, our study employed a warned reaction task that elicited anticipation of the valence of the emotional picture. The ACC may code for expected

Table 1. Significant activation during the delay period of each category of emotional picture in the expected condition compared to the delay period in the unexpected condition.

Area	BA	Side	t-score	x	y	z
Pleasant picture in the expected condition						
Middle frontal gyrus	9	L	8.36	−42	8	35
Cerebellum		R	8.05	17	−83	−38
Superior frontal gyrus	6	L	7.10	−10	20	50
Neutral picture in the expected condition						
Superior parietal lobule	7	L	6.36	−27	−60	48
Middle frontal gyrus	46	L	5.79	−45	24	24
Inferior frontal gyrus	44	L	5.25	−48	15	17
Unpleasant picture in the expected condition						
Inferior frontal gyrus	47	R	10.59	29	22	−10
Amygdala		R	5.95	29	−7	−13
Middle occipital gyrus	19	R	10.04	38	−65	9
Middle occipital gyrus	19	L	6.80	−38	−75	6
Anterior cingulate	32	L	6.46	−8	41	5
Medial frontal gyrus	10	R	6.23	3	53	11
Cuneus	17	R	6.29	12	−83	8
Lingual gyrus	17	L	6.24	−13	−82	0

Stereotaxic coordinates were derived from the atlas of Talairach and Tournoux [14].

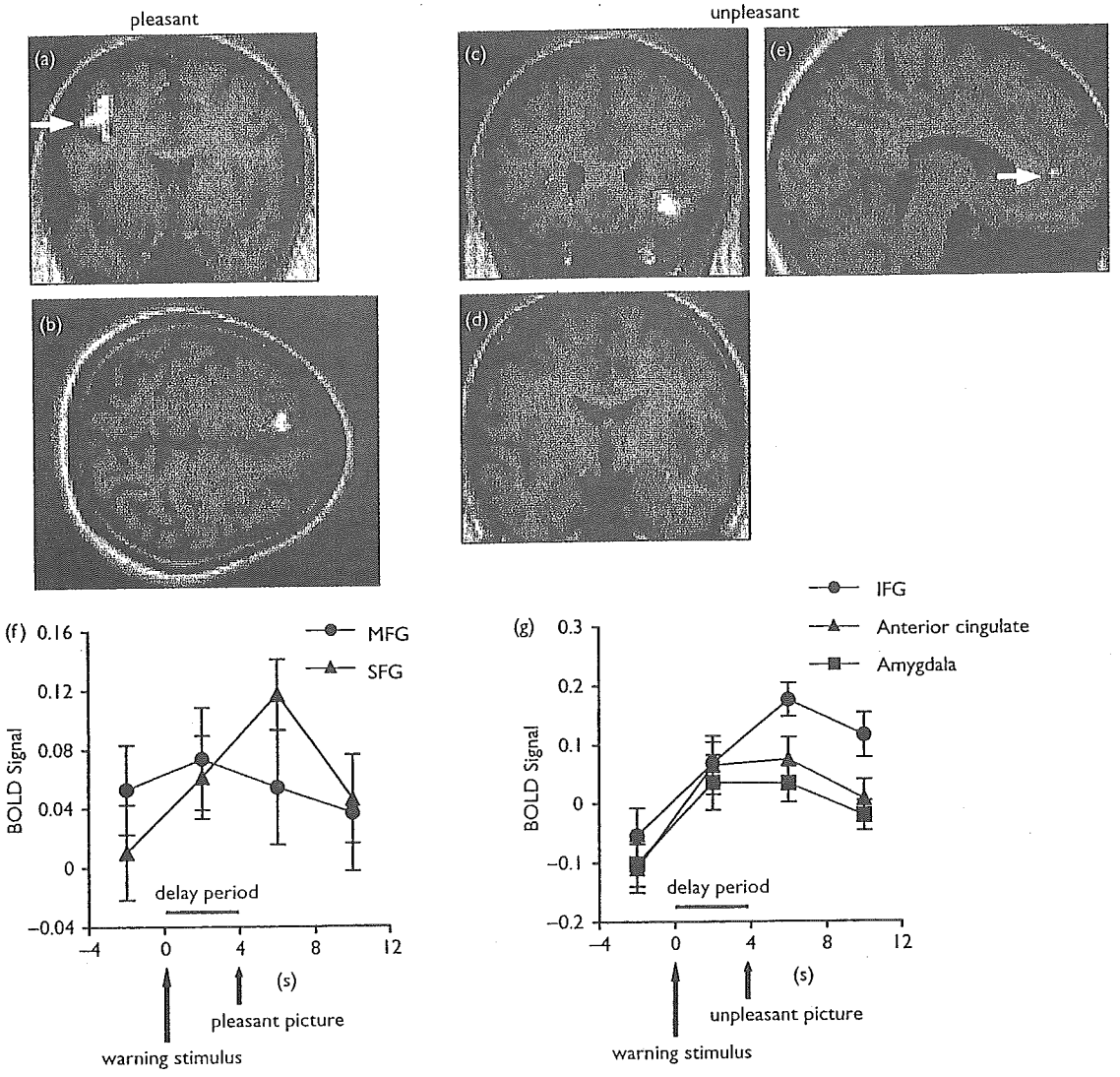

Fig. 2. Statistical parametric maps of brain regions (in the second level group analysis for the 15 subjects) showing significant increases in BOLD contrast associated with the delay period (**a,b**: pleasant, **c–e**: unpleasant) in the expected condition compared to the delay period in the unexpected condition at a statistical threshold of $p < 0.001$ (uncorrected) at the single voxel level and $p < 0.05$ (corrected) at the cluster level. Clusters of activation were overlaid onto a TI weighted anatomical magnetic resonance image. (a) Activation in the left middle frontal gyrus. (b) Activation in the left superior frontal gyrus. (c) Activation in the right inferior frontal gyrus. (d) Activation in the right amygdala. (e) Activation in the left anterior cingulate. (**f,g**) The BOLD signal time courses for the pre and post warning stimulus within the clusters in which there was significant activation during the expected condition (f: pleasant, g: unpleasant). MFG, middle frontal gyrus; SFG, superior frontal gyrus; IFG, inferior frontal gyrus. Error bars indicate s.e.m.

unpleasant emotional value. Thus our findings suggest that the amygdala and ACC participate in a neural circuit involved in the evaluation of the emotional significance of future information.

Another important finding of this study is that the primary visual cortex encompassing the cuneus and lingual gyrus were also activated during the expectancy of an unpleasant picture. The increased activity seen in perceptual processing areas before the input of negative stimuli implies that there is top-down processing from areas which are more anterior in the brain. The amygdala sends projections to the primary visual cortex and may play a modulatory role in the relatively early stages of sensory processing [24]. Posner and Raichle [25] suggested that a center in the ACC that may play an important role in priming the visual cortex for processing important input. Our data suggested that the input of negative information was modulated by the amygdala and ACC in order to effect an adaptive response.

CONCLUSION

The objective of this fMRI study was to examine the neural correlates of the expectancy of emotional stimuli carrying pleasant, unpleasant, or neutral content. In the expected

condition, compared with the unexpected condition, significant activation was observed in the medial, inferior and dorsolateral PFC. Whereas the expectancy of pleasant stimuli produced activation in the left dorsolateral and left medial PFC, and the right cerebellum, the expectancy of unpleasant stimuli produced activation in the right inferior and right medial PFC, the right amygdala, the left ACC, and in the bilateral visual cortex. These data suggest that left frontal activation is associated with the expectancy of pleasant stimuli and that right frontal activation is associated with the expectancy of unpleasant stimuli. Moreover, these findings suggest that the amygdala and ACC play a vital role in processing the expectancy of unpleasant stimuli and that the input of negative information is modulated by the amygdala and ACC in order to effect an adaptive response.

REFERENCES

1. Ekman P. *Cogn Emot* 6, 169–200 (1992).
2. LeDoux JE. In search of an emotional system in the brain: leaping from fear to emotion and consciousness. In: Gazzaniga MS (ed). *The Cognitive Neurosciences*. Cambridge: MIT Press; 1995, pp. 1049–1061.
3. LeDoux JE. Emotion. In: Plum F (ed). *Handbook of Physiology*. Bethesda: American Psychological Association; 1987, pp. 419–460.
4. Irwin W, Davidson RJ, Lowe MJ *et al. Neuroreport* 7, 1765–1769 (1996).
5. Reiman EM, Lane RD, Ahern GL *et al. Am J Psychiatry* 154, 918–925 (1997).
6. Taylor SF, Liberzon I, Fig LM *et al. Neuroimage* 8, 188–197 (1998).
7. Paradiso S, Johnson DL, Andreasen NC *et al. Am J Psychiatry* 156, 1618–1629 (1999).
8. Liberzon I, Taylor SF, Fig LM *et al. Neuropsychopharmacology* 23, 508–516 (2000).
9. Devinsky O, Morrell MJ and Vogt BA. *Brain* 118, 279–306 (1995).
10. Lane RD, Fink GR, Chau PM *et al. Neuroreport* 8, 3969–3972 (1997).
11. Whalen PJ, Bush G, McNally RJ *et al. Biol Psychiatry* 44, 1219–1228 (1998).
12. Lang PJ, Bradley MM, Fitzsimmons JR *et al. Psychophysiology* 35, 199–210 (1998).
13. Lang PJ, Bradley MM and Cuthbert BN. *International Affective Picture System (IAPS): Technical Manual and Affective Ratings*. Gainesville: University of Florida; 1999.
14. Talairach J and Tournoux P. *Co-planar Stereotaxic Atlas of the Human Brain*. Stuttgart: Thieme; 1988.
15. Lancaster JL, Woldorff MG, Parsons LM *et al. Hum Brain Mapp* 10, 120–131 (2000).
16. Pardo JV, Pardo PJ and Raichle ME. *Am J Psychiatry* 150, 713–719 (1993).
17. George MS, Ketter TA, Parekh PI *et al. Am J Psychiatry* 152, 341–351 (1995).
18. Teasdale JD, Howard RJ, Cox SG *et al. Am J Psychiatry* 156, 209–215 (1999).
19. Heller W. *Neuropsychology* 7, 476–489 (1993).
20. Davidson RJ. *Cogn Emot* 12, 307–330 (1998).
21. Baxter LR Jr, Schwartz JM, Phelps ME *et al. Arch Gen Psychiatry* 46, 243–250 (1989).
22. Aggleton JP, Kentridge RW and Sembi S. *Behav Brain Res* 48, 103–112 (1992).
23. Bush G, Luu P and Posner MI. *Trends Cogn Sci* 4, 215–222 (2000).
24. Amaral DG, Price JL, Pitkanen A *et al.* Anatomical organization of the primate amygdaloid complex. In: Aggleton JP (ed). *The Amygdala: Neurobiological Aspects of Emotion, Memory, and Mental Dysfunction*. New York: Wiley-Liss; 1992, pp. 1–66.
25. Posner MI and Raichle ME. *Behav Brain Sci* 18, 327–383 (1995).

Acknowledgements: This work was supported by a grant from Core Research for Evolutional Science and Technology (CREST), Japan Science and Technology Corporation (JST) and by a Health Science Research Grant for Research on Brain Science from the Ministry of Health, Welfare, and Labor of Japan.

Publisher's note: This offprint incorporates the errata published in NeuroReport, Volume 14.

nature neuroscience

Prediction of immediate and future rewards differentially recruits cortico-basal ganglia loops

Saori C Tanaka[1–3], Kenji Doya[1–3], Go Okada[3,4], Kazutaka Ueda[3,4], Yasumasa Okamoto[3,4] & Shigeto Yamawaki[3,4]

Evaluation of both immediate and future outcomes of one's actions is a critical requirement for intelligent behavior. Using functional magnetic resonance imaging (fMRI), we investigated brain mechanisms for reward prediction at different time scales in a Markov decision task. When human subjects learned actions on the basis of immediate rewards, significant activity was seen in the lateral orbitofrontal cortex and the striatum. When subjects learned to act in order to obtain large future rewards while incurring small immediate losses, the dorsolateral prefrontal cortex, inferior parietal cortex, dorsal raphe nucleus and cerebellum were also activated. Computational model–based regression analysis using the predicted future rewards and prediction errors estimated from subjects' performance data revealed graded maps of time scale within the insula and the striatum: ventroanterior regions were involved in predicting immediate rewards and dorsoposterior regions were involved in predicting future rewards. These results suggest differential involvement of the cortico-basal ganglia loops in reward prediction at different time scales.

In daily life, people make decisions based on the prediction of rewards at different time scales; for example, one might do daily exercise to achieve a future fitness goal, or resist the temptation of sweets to avoid future weight gain. Damage to the prefrontal cortex often impairs daily decision making, which requires assessment of future outcomes[1,2]. Lesions in the core of the nucleus accumbens in rats result in a tendency to choose small immediate rewards over larger future rewards[3]. Low activity of the central serotonergic system is associated with impulsive behavior in humans[4], and animals with lesions in the ascending serotonergic pathway tend to choose small immediate rewards over larger future rewards[5,6]. A possible mechanism underlying these observations is that different sub-loops of the topographically organized cortico-basal ganglia network are specialized for reward prediction at different time scales and that they are differentially activated by the ascending serotonergic system[7]. To test whether there are distinct neural pathways for reward prediction at different time scales, we developed a 'Markov decision task' in which an action affects not only the immediate reward but also future states and rewards. Using fMRI, we analyzed brain activity in human subjects as they performed this task. Recent functional brain imaging studies have shown the involvement of specific brain areas, such as the orbitofrontal cortex (OFC) and the ventral striatum, in prediction and perception of rewards[8–11]. In these previous studies, however, rewards were given either independent of the subject's actions or as a function of the current action. Our Markov decision task probes decision making in a dynamic context, with small losses followed by a large positive reward. The results of the block-design analysis suggest differential involvement of brain areas in decision making by prediction of rewards at different time scales. By analyzing subjects' performance data according to a theoretical model of reinforcement learning, we found a gradient of activation within the insula and the striatum for prediction of rewards at different time scales.

RESULTS

Behavioral results

In the Markov decision task, a visual signal (one of three shapes) was presented at the start of each trial to indicate one of three states, and the subject selected one of two actions: pressing the right or left button with the right hand (Fig. 1a; see Methods for details). For each state, the subject's action choice affected not only the immediate reward, but also the state subsequently presented (Fig. 1b,c).

The rule of state transition was fixed during the entire experiment (Fig. 1), but the rules of reward delivery changed according to the task condition. In the SHORT condition, action a_1 gives a small positive reward ($+r_1$ = 20 yen average; see Methods) and action a_2 gives a small loss ($-r_1$) in all three states (Fig. 1b). The optimal behavior for maximizing total reward in the SHORT condition is to collect small positive rewards by taking action a_1 at each state. In the LONG condition, action a_2 at state s_3 gives a big bonus ($+r_2$ = 100 yen average; see Methods), and action a_1 at state s_1 results in a big loss ($-r_2$; Fig. 1c). The optimal behavior is to receive small losses at state s_1 and s_2 to obtain a large positive reward at state s_3 by taking action a_2 at each state; this is opposite to the optimal behavior in the SHORT condition. Whereas the optimal strategy in the SHORT condition results in small, immediate rewards at each step, the optimal strategy in the LONG condition results in small immediate losses but a net positive reward by the end of one cycle. Thus, for successful action in the LONG condition, subjects must consider both the

[1]Department of Bioinformatics and Genomics, Nara Institute of Science and Technology, 8916-5 Takayama, Ikoma, Nara 630-0101, Japan. [2]Department of Computational Neurobiology, ATR Computational Neuroscience Laboratories, 2-2-2 Hikaridai, Keihanna Science City, Kyoto 619-0288, Japan. [3]CREST, Japan Science and Technology Agency, 2-2-2 Hikaridai, Keihanna Science City, Kyoto 619-0288, Japan. [4]Department of Psychiatry and Neurosciences, Hiroshima University, 1-2-3 Kasumi, Minamiku, Hiroshima 734-8551, Japan. Correspondence should be addressed to K.D. (doya@atr.jp).

Published online 4 July 2004; doi:10.1038/nn1279

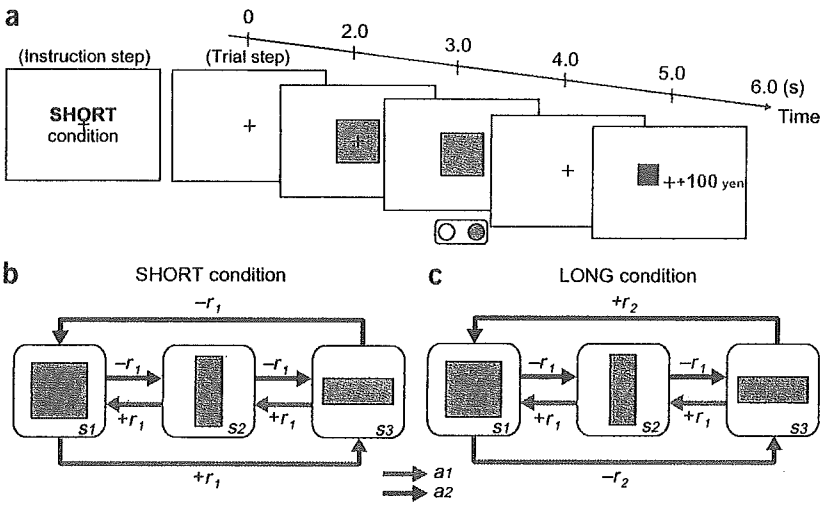

Figure 1 Experimental design. (a) Sequences of stimulus and response events in the task. At the beginning of each condition block, the condition is informed by displaying text (6 s), such as 'SHORT condition' (instruction step). In each trial step, a fixation point is presented on the screen, and after 2 s, one of three shapes (square, vertical rectangle or horizontal rectangle) is presented for 1 s. As the fixation point vanishes after 1 s, the subject presses either the right or left button within 1 s. After a short delay (1 s), a reward for that action is presented by a number (indicating yen gained or lost) and the past cumulative reward is shown by a bar graph. Thus, one trial step takes 6 s. (b,c) The rules of the reward and state transition for action a_1 (magenta arrows) and action a_2 (blue arrows) in the SHORT (b) and LONG (c) conditions. The small reward r_1 was 10, 20 or 30 yen, with equal probability, and the large reward r_2 was 90, 100, or 110 yen. The rule of state transition was the same for all conditions: $s_3 \rightarrow s_2 \rightarrow s_1 \rightarrow s_3 \ldots$ for action a_1, and $s_1 \rightarrow s_2 \rightarrow s_3 \rightarrow s_1 \rightarrow \ldots$ for action a_2. Although the optimal behaviors are opposite (SHORT: a_1; LONG: a_2), the expected cumulative reward during one cycle of the optimal behavior is 60 yen in both the SHORT ($+20 \times 3$) and LONG (-20, -20, $+100$) conditions.

immediate reward and the future reward expected from the subsequent state, and for success in the SHORT condition, subjects need to consider only the immediate outcome of their actions. Subjects performed 15 trials in a SHORT condition block and 15 trials in a LONG condition block. There were also two control conditions, NO (reward was always zero) and RANDOM (reward was $+r_1$ or $-r_1$, regardless of state or action), so a total of four condition blocks were performed (see Fig. 2a for task schedule).

All subjects successfully learned the optimal behaviors: taking action a_1 in the SHORT condition (Fig. 2b) and action a_2 in the LONG condition (Fig. 2c). Cumulative rewards within each SHORT block (Fig. 2d) and LONG block (Fig. 2e) also indicate successful learning. It can be seen from the single-subject data in the LONG condition (Fig. 2e, orange) that the subject learned to lose small amounts ($-r_1$) twice to get a big bonus ($+r_2$). The average cumulative reward in the last block was 254 yen in the SHORT condition and 257 yen in the LONG condition, which was 84.7% and 85.7%, respectively, of the theoretical optimum of 300 yen.

Block-design analysis

To find the brain areas that are involved in immediate reward prediction, we compared brain activity during the SHORT condition and the NO condition, in which reward was always zero. In the SHORT versus NO contrast, a significant increase in activity was observed in the lateral OFC (Fig. 3a), the insula and the occipitotemporal area (OTA) (Fig. 3b), as well as in the striatum, the globus pallidus (GP) (Fig. 3c) and the medial cerebellum (Fig. 3d) (threshold of $P < 0.001$, uncorrected for multiple comparisons). These areas may be involved in reward prediction based on immediate outcome.

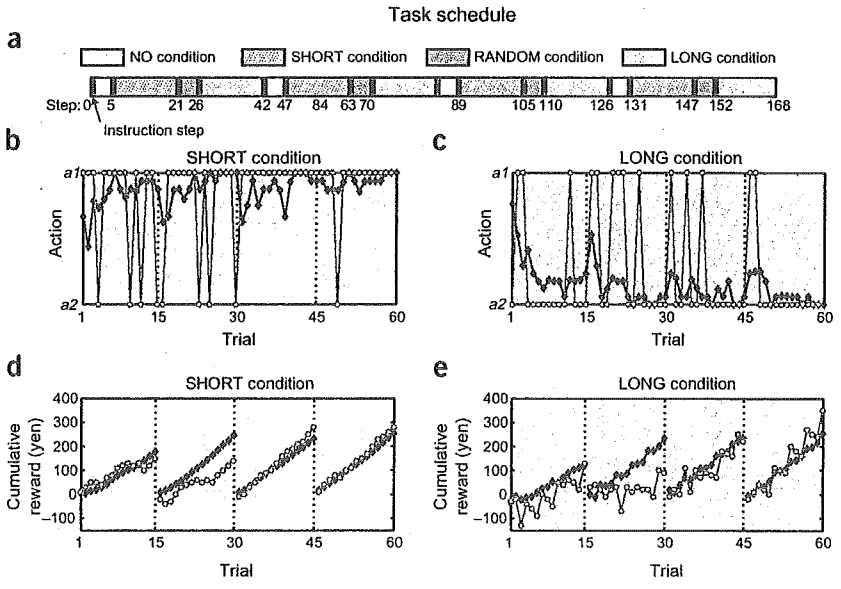

Figure 2 Task schedule and behavioral results. (a) A set of four condition blocks—NO (4 trials), SHORT (15 trials), RANDOM (4 trials), LONG (15 trials)—was repeated four times. At the beginning of each condition block, the task condition was presented to the subject (instruction step); thus, the entire experiment consisted of 168 steps (152 trial steps and 16 instruction steps). (b,c) The selected action of a representative single subject (orange) and the group average ratio of selecting a_1 (blue) in the (b) SHORT and (c) LONG conditions. (d,e) The accumulated reward in each block of a representative single subject (orange) and the group average (blue) in the (d) SHORT and (e) LONG conditions. To clearly show the learning effects, data from four trial blocks in the SHORT and LONG conditions are concatenated, with the dotted lines indicating the end of each condition block.

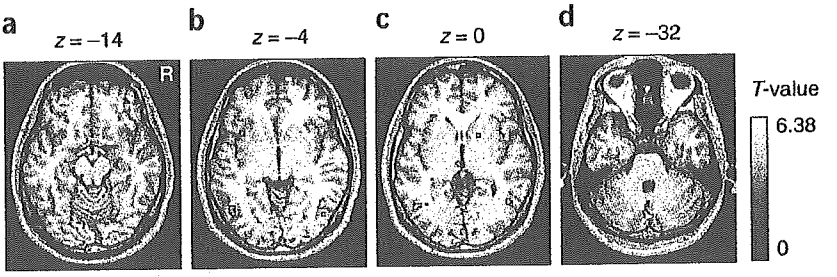

Figure 3 Brain areas activated in the SHORT versus NO contrast ($P < 0.001$, uncorrected; extent threshold of four voxels). (a) Lateral OFC. (b) Insula. (c) Striatum. (d) Medial cerebellum.

To identify areas involved in future reward prediction, we compared the brain activity during LONG and SHORT conditions. In the LONG versus SHORT contrast, a robust increase in activity was observed in the ventrolateral prefrontal cortex (VLPFC), the insula, the dorsolateral prefrontal cortex (DLPFC), the dorsal premotor cortex (PMd), the inferior parietal cortex (IPC) (Fig. 4a), the striatum, GP (Fig. 4b), the dorsal raphe nucleus (Fig. 4c), the lateral cerebellum (Fig. 4d), the posterior cingulate cortex and the subthalamic nucleus ($P < 0.001$, uncorrected). Activity in the striatum was highly significant (threshold at $P < 0.05$, corrected for a small volume when using an anatomically defined region of interest (ROI) in the striatum; see Methods). These areas are specifically involved in decision making based on the prediction of reward in multiple steps in the future. In the LONG versus NO contrast, the activated areas were approximately the union of the areas activated in the SHORT versus NO and LONG versus SHORT contrasts. These results were consistent with our expectation that both immediate and future reward prediction were required in the LONG condition. The results of block-design analysis, including the LONG versus NO contrast, are summarized in Supplementary Table 1 online. Activitions in both SHORT and LONG conditions were stronger in the first two blocks, when subjects were involved in active trial and error, than in the last two blocks when the subjects' behavior became repetitive.

We compared the activitions in the SHORT versus NO contrast and the LONG versus SHORT contrast, and observed that three regions showed significant activity in both contrasts: the lateral prefrontal cortex (lateral OFC and VLPFC), the insula and the anterior striatum (Fig. 5). In the lateral PFC (Fig. 5a), although the activities in lateral OFC for the SHORT versus NO contrast (red) and in the VLPFC for the LONG versus SHORT contrast (blue) were close in location, they were clearly separated on the cortical surface. Activities in the insula were also separated (Fig. 5b). In the anterior striatum (Fig. 5c), we found limited overlaps between the two contrasts (green). In all three areas, activations in the SHORT versus NO contrast were found in the ventral parts, whereas activations in the LONG versus SHORT contrast were found in the dorsal parts.

These results of block-design analysis suggest differential involvement of brain areas in predicting immediate and future rewards.

Performance-based multiple regression analysis

To further clarify the brain structures specific to reward prediction at different time scales, we estimated how much reward the subjects should have predicted on the basis of their performance data and used their time courses as the explanatory variables of regression analysis. We took the theoretical framework of temporal difference (TD) learning[12], which has been successfully used for explaining reward-predictive activations of the midbrain dopaminergic system as well as those of the cortex and the striatum[8,11,13–16]. In TD learning theory, the predicted amount of future reward starting from a state $s(t)$ is formulated as the 'value function'

$$V(t) = E[r(t+1) + \gamma r(t+2) + \gamma^2 r(t+3) + \ldots]. \quad (1)$$

Any deviation from the prediction is given by the TD error

$$\delta(t) = r(t) + \gamma V(t) - V(t-1), \quad (2)$$

which is a crucial learning signal for reward prediction and action selection. The 'discount factor' γ ($0 \leq \gamma < 1$) controls the time scale of prediction: when $\gamma = 0$, only the immediate reward $r(t+1)$ is considered, but as γ approaches 1, rewards in the further future are taken into account.

We estimated the time courses of reward prediction $V(t)$ and prediction error $\delta(t)$ from each subject's performance data and used them as the explanatory variables in multiple regression analysis with fMRI data (see Methods). In our Markov decision task, the minimum value of γ needed to find the optimal action in the LONG condition is 0.36, and any small value of γ is sufficient in the SHORT condition. From the results of our block-design analysis, we assumed that different networks involving the cortex and basal ganglia are specialized for reward prediction at different time scales and that they work in parallel, depending on the requirement of the task. Thus, we varied the discount factor γ as 0, 0.3, 0.6, 0.8, 0.9 and 0.99: small γ for immediate reward prediction and large γ for long future reward prediction. An example of these time courses is shown in Supplementary Figure 1 online.

We observed a significant correlation with reward prediction $V(t)$ in the medial prefrontal cortex (mPFC; including the anterior cingulate cortex (ACC) and the medial OFC) (Fig. 6a) and bilateral insula (Fig. 6b), left hippocampus and left temporal pole ($P < 0.001$, uncorrected; see Supplementary Table 2 online). Figure 6 shows the correlated

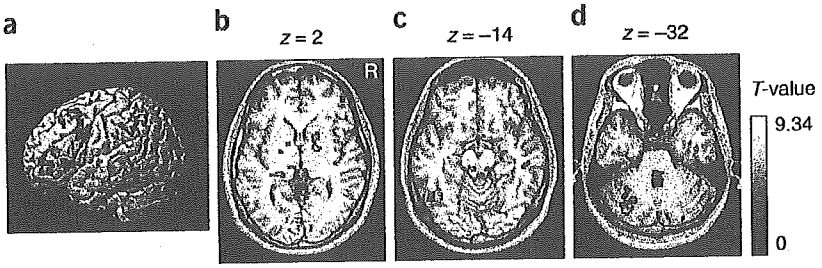

Figure 4 Brain areas activated in the LONG versus SHORT contrast ($P < 0.0001$, uncorrected; extent threshold of four voxels for illustration purposes). (a) DLPFC, IPC, PMd. (b) GP, striatum. (c) Dorsal raphe nucleus. (d) Left lateral cerebellum.

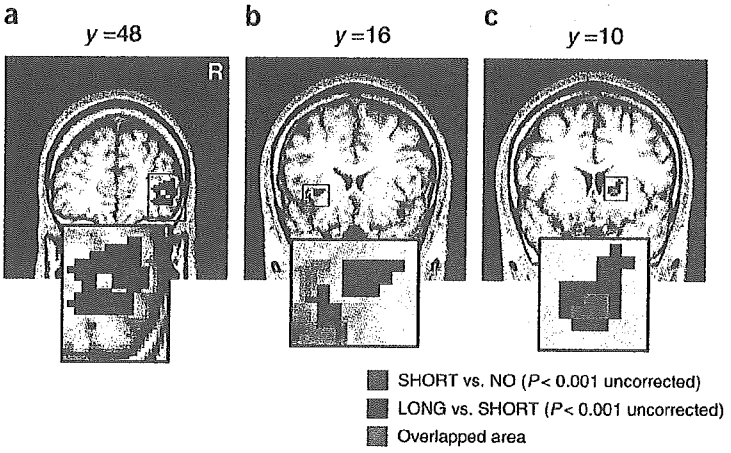

Figure 5 Comparison of brain areas activated in the SHORT versus NO contrast (red) and the LONG versus SHORT contrast (blue). (**a–c**) These figures show activation maps focused on (**a**) the lateral OFC (red (*x*, *y*, *z*) = (38, 46, −14); blue (46, 47, 3)) (**b**) the insula (red (−36, 13, −4); blue (−30, 18, 1)), and (**c**) the striatum (red (18, 10, 0); blue (18, 12, 3)) where we observed significant activation in both contrasts. The areas where activity overlapped area are shown in green.

voxels within these areas using a gradient of colors for different γ values (red for $\gamma = 0$, blue for $\gamma = 0.99$). Activity in the mPFC, temporal pole and hippocampus correlated with reward prediction with a longer time scale ($\gamma \geq 0.6$). Furthermore, in the insula, we found a graded map of activity for reward prediction at different time scales (Fig. 6b). Whereas activity in the ventroanterior region correlated with reward prediction at a shorter time scale, activity in the dorsoposterior region correlated with reward prediction at a longer time scale.

We also found, in the basal ganglia, significant correlation with reward prediction error $\delta(t)$ using a wide range of time scales (Fig. 6c; $P < 0.001$, uncorrected; see **Supplementary Table 3** online and Methods). Again, we found a graded map, which had a short time scale in the ventroanterior part and a long time scale in the dorsoposterior part. The coincidence of the ventroanterior-dorsoposterior maps and the ventroanterior-dorsoposterior shifts in activities (Fig. 6b,c) indicate that, while the ventroanterior regions with smaller γ were predominantly active in the SHORT condition, the dorsoposterior regions with larger γ became more active in the LONG condition.

DISCUSSION

The results of the block-design and performance-based regression analyses suggest differential involvement of brain areas in action learning by prediction of rewards at different time scales. Both block-design and performance-based regression analyses showed activity in the insula and the anterior striatum. Activations of the ventral region in the SHORT versus NO contrast and the dorsal region in the LONG versus SHORT contrast in each area (Fig. 5) are consistent with the ventroanterior-dorsoposterior maps of the discount factor γ found in performance-based regression analysis (Fig. 6).

The insula takes a pivotal position in reward processing by receiving primary taste and visceral sensory input[17] and sending output to the OFC[18] and the striatum[19]. Previous studies showed that the insula is activated with anticipation of primary reward[10] and that insular lesion causes deficits in incentive learning for primary reward[20]. Our results confirm the role of the insula in prediction of non-primary, monetary reward[21], and further suggest heterogeneous organization within the insula. Previous imaging studies also showed involvement of the insula, especially the ventroanterior region, in processing aversive outcomes[22,23]. Thus a possible interpretation of the activation of the insula in the LONG condition is that it

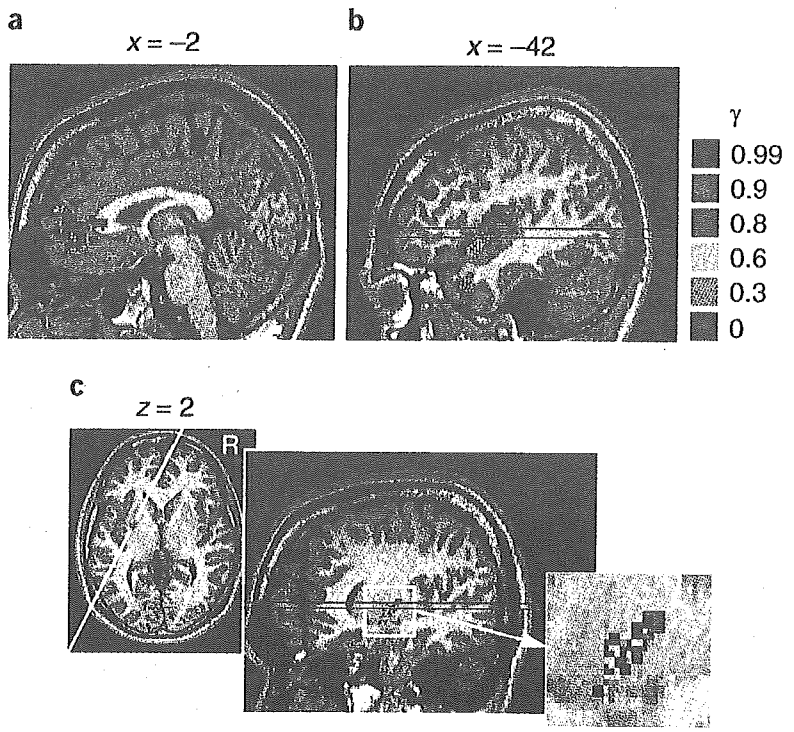

Figure 6 Voxels with a significant correlation (height threshold $P < 0.001$, uncorrected; extent threshold of four voxels) with reward prediction $V(t)$ and prediction error $\delta(t)$ are shown in different colors for different settings of the discount factor γ. Voxels correlated with two or more regressors are shown by a mosaic of colors. (**a**, **b**) Significant correlation with reward prediction $V(t)$. (**a**) mPFC. (**b**) Insula. (**c**) Significant correlation with reward prediction error $\delta(t)$ restricted to ROI in the striatum (slice at white line in horizontal slice at $z = 2$ mm). Note the ventroanterior-to-dorsoposterior gradient with the increase in γ both in the insula and the striatum. Red and blue lines correspond to the *z*-coordinate levels of activation peaks in the insula and striatum shown in **Figure 5b,c** (red for the SHORT versus NO and blue for the LONG versus SHORT contrasts).

reflected the losses that subjects acquired before getting a large reward. However, we also ran a regression analysis using losses and found significant correlation in the ventroanterior region of the insula. Anatomical and physiological studies of the insula also showed involvement of its ventroanterior part in perception of aversive stimuli[17]. Thus we argue that the activation of dorsoposterior insula is not simply due to losses in the LONG condition.

Previous brain imaging and neural recording studies suggest a role for the striatum in prediction and processing of reward[9,10,14,21,24–29]. Consistent with previous fMRI studies[8,11,16], our results showed striatal activity correlated with the error of reward prediction. Reinforcement learning models of the basal ganglia[13–15] posit that the striatum learns reward prediction and action selection based on the reward prediction error $\delta(t)$ represented by the dopaminergic input. Correlation of striatal activity with reward prediction error $\delta(t)$ could be due to dopamine-dependent plasticity of cortico-striatal synapses[30].

In lateral OFC, DLPFC, PMd, IPC and dorsal raphe, we found significant activations in the block-design analyses, but we did not find strong correlation in regression analyses. This may be because these areas perform functions that are helpful for reward prediction and action selection, but their activities do not directly represent the amount of predicted reward or prediction error at a specific time scale.

In reinforcement learning theory, an optimal action selection is realized by taking the action a that maximizes the 'action value' $Q(s, a)$ at a given state s. The action value is defined as $Q(s, a) = E[\, r(s, a) + \gamma\, V(s'(s, a))]$ and represents the expected sum of the immediate reward $r(s, a)$ and the weighted future rewards $V(s'(s, a))$, where $s'(s, a)$ means the next state reached by taking an action a at a state s (refs. 12,15). According to this framework, we can see that prediction of immediate reward $r(s, a)$ is helpful for action selection based on rewards at either short or long time scales, that is, with any value of the discount factor γ. On the other hand, prediction of state transition $s'(s, a)$ is helpful only in long-term reward prediction with positive values of γ.

In the lateral OFC, we observed significant activity in both the SHORT versus NO and the LONG versus NO contrasts (Supplementary Table 1 online), but no significant correlation with reward prediction $V(t)$ or reward prediction error $\delta(t)$ in regression analysis. This suggests that the lateral OFC takes the role of predicting immediate reward $r(s, a)$, which is used for action selection in both SHORT and LONG conditions, but not in the NO condition. This interpretation is consistent with previous studies demonstrating the OFC's role in prediction of rewards, immediately following sensorimotor events[31,32], and action selection based on reward prediction[23,33,34].

In the DLPFC, PMd and IPC, there were significant activations in both the LONG versus NO and the LONG versus SHORT contrasts (Supplementary Table 1 online) but no significant correlation with either $V(t)$ or $\delta(t)$. A possible interpretation is that this area is involved in prediction of future state $s'(s, a)$ in the LONG condition but not in the SHORT or NO conditions. This interpretation is consistent with previous studies showing the role of these cortical areas in imagery[35], working memory and planning[36,37].

The dorsal raphe nucleus was activated in the LONG versus SHORT contrast, but was not correlated with $V(t)$ or $\delta(t)$. In consideration of its serotonergic projection to the cortex and the striatum and serotonin's implication with behavioral impulsivity[4–6], a possible role for the dorsal raphe nucleus is to control the effective time scale of reward prediction[7]. Its higher activity in the LONG condition, where a large setting of γ is necessary, is consistent with this hypothesis.

Let us consider the present experimental results in light of the anatomy of cortico-basal ganglia loops (illustrated in Supplementary Fig. 2). The cortex and the basal ganglia both have parallel loop organization, with four major loops (limbic, cognitive, motor and oculomotor) and finer, topographic sub-loops within each major loop[38]. Our results suggest that the areas within the limbic loop[39], namely the lateral OFC and ventral striatum, are involved in immediate reward prediction. On the other hand, areas within the cognitive and motor loops[38], including the DLPFC, IPC, PMd and dorsal striatum, are involved in future reward prediction. The connections from the insula to the striatum are topographically organized, with the ventral-anterior, agranular cortex projecting to the ventral striatum and the dorsal-posterior, granular cortex projecting to the dorsal striatum[19] (see Supplementary Fig. 2). The graded maps shown in Figure 6b,c are consistent with this topographic cortico-striatal organization and suggest that areas that project to the more dorsoposterior part of the striatum are involved in reward prediction at a longer time scale. These results are consistent with the observations that localized damages within the limbic and cognitive loops manifest as deficits in evaluation of future rewards[1,3,34,40,41] and learning of multi-step behaviors[42]. The parallel learning mechanisms in the cortico-basal ganglia loops used for reward prediction at a variety of time scales may have the merit of enabling flexible selection of a relevant time scale appropriate for the task and the environment at the time of decision making.

A possible mechanism for selection or weighting of different cortico-basal ganglia loops with an appropriate time scale is serotonergic projection from the dorsal raphe nucleus[7] (see Supplementary Fig. 2), which was activated in the LONG versus SHORT contrast. Although serotonergic projection is supposed to be diffuse and global, differential expression of serotonergic receptors in the cortical areas and in the ventral and dorsal striatum[43,44] would result in differential modulation. The mPFC, which had significant correlation with reward prediction $V(t)$ at long time scales ($\gamma \geq 0.6$), may regulate the activity of the raphe nucleus through reciprocal connection[45,46]. This interpretation is consistent with previous studies using tasks that require long-range prospects for problem solving, such as the gambling problem[1] or delayed reward task[2], which showed involvement of the medial OFC. Future studies using the Markov decision task under pharmacological manipulation of the serotonergic system should clarify the role of serotonin in regulating the time scale of reward prediction.

Recent brain imaging and neural recording studies report involvement of a variety of cortical areas and the striatum in reward processing[8–11,16,21,23–29,32,33,47–49]. Although some neural recording studies have used experimental tasks that require multiple trial steps for getting rewards[47,48], none of the previous functional brain imaging studies addressed the issue of reward prediction at different time scales, and considered only rewards immediately following stimuli or actions. We were able extract specific functions of OFC, DLPFC, mPFC, insula and cortico-basal ganglia loops using our new Markov decision task and a reinforcement learning model–based regression analysis. Our regression analysis not only extracted brain activities specific to reward prediction, but also revealed a topographic organization in reward prediction (Fig. 6). The combination of our Markov decision task with event-related fMRI and magnetoencephalography (MEG) should further clarify the functions used for reward prediction and perception at different time scales, and at finer spatial and temporal resolutions.

METHODS

Subjects. Twenty healthy, right-handed volunteers (18 males and 2 females, ages 22–34 years) gave informed consent to participate in the experiment, which was conducted with the approval of the ethics and safety committees of Advanced Telecommunication Research Institute International (ATR) and Hiroshima University.

Behavioral task. In the Markov decision task (Fig. 1), one of three states was visually presented to the subject using three different shapes, and the subject selected one of two actions by pressing one of two buttons using their right hand (Fig. 1a). The rule of state transition was the same for all conditions: $s_3 \rightarrow s_2 \rightarrow s_1 \rightarrow s_3 \ldots$ for action a_1, and $s_1 \rightarrow s_2 \rightarrow s_3 \rightarrow s_1 \rightarrow \ldots$ for action a_2. The rules for reward, however, changed in each condition. In the SHORT condition (Fig. 1b), action a_1 results in a small positive reward ($+r_1$ = 10, 20 or 30 yen, with equal probabilities), whereas action a_2 results in a small loss ($-r_1$) at any of the three states. Thus, the optimal behavior is to collect small positive rewards at each state by performing action a_1. In the LONG condition (Fig. 1c), however, the reward setting is such that action a_2 gives a large positive reward ($+r_2$ = 90, 100 or 110 yen) at state s_3, and action a_1 gives a large loss ($-r_2$) at state s_1. Thus, the optimal behavior is to receive small losses at states s_1 and s_2 to obtain a large positive reward at state s_3 by taking action a_2 at each state. There were two control conditions: the NO condition, where the reward was always zero, and the RANDOM condition, where the reward was positive ($+r_1$) or negative ($-r_1$) with equal probability, regardless of state or action.

Subjects completed 4 trials in a NO condition block, 15 trials in a SHORT condition block, 4 trials in a RANDOM condition block and 15 trials in a LONG condition block. A set of four condition blocks (NO, SHORT, RANDOM, LONG) was repeated four times (Fig. 2a). Subjects were informed of the current condition at the beginning of each condition block by text on the screen (first slide in Fig. 1a); thus, the entire experiment consisted of 168 steps (152 trial steps and 16 instruction steps), taking about 17 min. The mappings of the three states to the three figures, and the two buttons to the two actions, were randomly set at the beginning of each experiment, so that subjects were required to learn the amount of reward associated with each figure-button pair in both SHORT and LONG conditions. Furthermore, in the LONG condition, subjects had to learn the subsequent figure for each figure-action pair and take into account the amount of reward expected from the subsequent figure in selecting a button.

fMRI imaging. A 1.5-tesla scanner (Shimadzu-Marconi, Magnex Eclipse) was used to acquire both structural T1-weighted images (repetition time, TR = 12 ms, TE = 4.5 ms, flip angle = 20°, matrix = 256 × 256, FoV = 256 mm, thickness = 1 mm, slice ga$P$ = 0 mm) and T2*-weighted echo planar images (TR = 6 s, TE = 55 ms, flip angle = 90°, 50 transverse slices, matrix = 64 × 64, FoV = 192 mm, thickness = 3 mm, slice gap = 0 mm) showing blood oxygen level–dependent (BOLD) contrasts.

Because the aim of the present study was to identify brain activity underlying reward prediction over multiple trial steps, we acquired functional images every 6 s (TR = 6 s), in synchrony with single trials. Although shorter TRs and event-related designs are often used in experiments that aim to distinguish brain responses to events within a trial[9,11,21,26], analysis of those finer events in time were not the focus of the current study. With this longer TR, the BOLD signal in a single scan contained a mixture of responses for a reward-predictive stimulus and reward feedback. However, because of the progress of learning and the stochastic nature of the amount of reward, the time courses of reward prediction $V(t)$ and prediction error $\delta(t)$ over the 168 trial steps were markedly different. Thus, we could separate activity corresponding to reward prediction from that corresponding to outcomes by using both reward prediction $V(t)$ and reward outcome $r(t)$ in multiple regression analysis, as described below.

Data analysis. The data were pre-processed and analyzed with SPM99 (www.fil.ion.ucl.ac.uk/spm/spm99.html). The first two volumes of images were discarded to avoid T1 equilibrium effects. The images were realigned to the first image as a reference, spatially normalized with respect to the Montreal Neurological Institute EPI template, and spatially smoothed with a Gaussian kernel (8 mm, full-width at half-maximum).

We conducted two types of analysis. One was block-design analysis using four boxcar regressors covering the whole experiment, convolved with a hemodynamic response function as the reference waveform for each condition (NO, SHORT, RANDOM, LONG). We did not find substantial differences between SHORT versus NO and SHORT versus RANDOM contrasts, or between LONG versus NO and LONG versus RANDOM contrasts. Therefore we report here only the results with the NO condition as the control condition. The other method was multivariate regression analysis using explanatory variables, representing the time course of the reward prediction $V(t)$ or reward prediction error $\delta(t)$ at six different timescales γ, estimated from subjects' performance data (described below).

In both analyses, images of parameter estimates for the contrast of interest were created for each subject. These were then entered into a second-level group analysis using a one-sample t test at a threshold of $P < 0.001$, uncorrected for multiple comparisons (random effects analysis) and extent threshold of four voxels. Small-volume correction (SVC) was done at a threshold of $P < 0.05$ using an ROI within the striatum (including the caudate and putamen), which was defined anatomically based on a normalized T1 image.

Procedures of performance-based regression analysis. The time courses of reward prediction $V(t)$ and reward prediction error $\delta(t)$ were estimated from each subject's performance data—state $s(t)$, action $a(t)$ and reward $r(t)$—as described below.

Reward prediction. To estimate how much of a forthcoming reward a subject would have expected at each step during the Markov decision task, we took the definition of the value function (equation 1) and reformulated it based on the recursive structure of the task. Namely, if the subject starts from a state $s(t)$ and comes back to the same state after k steps, the expected cumulative reward $V(t)$ should satisfy the consistency condition $V(t) = r(t + 1) + \gamma\, r(t + 2) + \ldots + \gamma^{k-1} r(t + k) + \gamma^k V(t)$.

Thus, for each time t of the data file, we calculated the weighted sum of the rewards acquired until the subject returned to the same state and estimated the value function for that episode as

$$\hat{V}(t) = \frac{\left[r(t+1) + \gamma r(t+2) + \Lambda + \gamma^{k-1} r(t+k)\right]}{1-\gamma^k} \qquad (1)$$

The estimate of the value function $V(t)$ at time t was given by the average of all previous episodes from the same state as at time t

$$V(t) = \frac{1}{L}\sum_{l=1}^{L} \hat{V}(t_l) \qquad (2)$$

where $\{t_1, \ldots, t_L\}$ are the indices of time visiting the same state as $s(t)$, that is, $s(t_1) = \ldots = s(t_L) = s(t)$.

Reward prediction error. The TD error (equation 2) was calculated from the difference between the actual reward $r(t)$ and the temporal difference of the estimated value function $V(t)$.

We separately calculated the time courses of $V(t)$ and $\delta(t)$ during SHORT and LONG conditions; we concatenated data of four blocks in the SHORT condition, and calculated $V(t)$ and $\delta(t)$ as described above. We used the same process for the LONG condition data. During the NO and RANDOM conditions, the values of $V(t)$ and $\delta(t)$ were fixed at zero. Finally, we reconstructed the data corresponding to the real time course of the experiment. Examples of the time course of these variables are shown in **Supplementary Figure 1** online. We used either $V(t)$ or $\delta(t)$ as the explanatory variable in a regression analysis by SPM. To remove any effects of factors other than reward prediction, we concurrently used other variables in the regression, namely the four box-car functions representing each condition (NO, SHORT, RANDOM, LONG). Because the immediate reward prediction $V(t)$ with $\gamma = 0$ can coincide with reward outcome $r(t)$ if learning is perfect, we included the reward outcome $r(t)$ in regression analyses with $V(t)$. Thus, the significant correlation with $V(t)$ (**Fig. 6a,b**) should represent a predictive component rather than a reward outcome.

The amplitude of explanatory variables $\delta(t)$ with all γ were large in early trials and decreased as subjects learned the task (**Supplementary Fig. 1** online). This decreasing trend causes a risk that areas that are activated early in trials, such as those responsible for general attentiveness or novelty, have correlations with $\delta(t)$. Because our aim in regression analysis was to clarify the brain structures involved in reward prediction at specific time scales, we removed the areas that had similar correlation to $\delta(t)$ at all settings of γ from considerations in **Figure 6** and **Supplementary Table 3** online. To compare the results of regression analysis

with six different values of γ, we used display software that can overlay multiple activation maps in different colors on a single brain structure image. When a voxel is significantly activated in multiple values of γ, it is shown by a mosaic of multiple colors, with apparent subdivision of the voxel (Fig. 6).

Note: Supplementary information is available on the Nature Neuroscience website.

ACKNOWLEDGMENTS

We thank K. Samejima, N. Schweighofer, M. Haruno, H. Imamizu, S. Higuchi, T. Yoshioka, T. Chaminade and M. Kawato for helpful discussions and technical advice. This research was funded by 'Creating the Brain,' Core Research for Evolutional Science and Technology (CREST), Japan Science and Technology Agency.

COMPETING INTERESTS STATEMENT

The authors declare that they have no competing financial interests.

Received 5 March; accepted 2 June 2004
Published online at http://www.nature.com/natureneuroscience/

1. Bechara, A., Damasio, H. & Damasio, A.R. Emotion, decision making and the orbitofrontal cortex. *Cereb. Cortex* **10**, 295–307 (2000).
2. Mobini, S. *et al.* Effects of lesions of the orbitofrontal cortex on sensitivity to delayed and probabilistic reinforcement. *Psychopharmacology (Berl.)* **160**, 290–298 (2002).
3. Cardinal, R.N., Pennicott, D.R., Sugathapala, C.L., Robbins, T.W. & Everitt, B.J. Impulsive choice induced in rats by lesions of the nucleus accumbens core. *Science* **292**, 2499–2501 (2001).
4. Rogers, R.D. *et al.* Dissociable deficits in the decision-making cognition of chronic amphetamine abusers, opiate abusers, patients with focal damage to prefrontal cortex, and tryptophan-depleted normal volunteers: evidence for monoaminergic mechanisms. *Neuropsychopharmacology* **20**, 322–339 (1999).
5. Evenden, J.L. & Ryan, C.N. The pharmacology of impulsive behaviour in rats: the effects of drugs on response choice with varying delays of reinforcement. *Psychopharmacology (Berl.)* **128**, 161–170 (1996).
6. Mobini, S., Chiang, T.J., Ho, M.Y., Bradshaw, C.M. & Szabadi, E. Effects of central 5-hydroxytryptamine depletion on sensitivity to delayed and probabilistic reinforcement. *Psychopharmacology (Berl.)* **152**, 390–397 (2000).
7. Doya, K. Metalearning and neuromodulation. *Neural Net.* **15**, 495–506 (2002).
8. Berns, G.S., McClure, S.M., Pagnoni, G. & Montague, P.R. Predictability modulates human brain response to reward. *J. Neurosci.* **21**, 2793–2798 (2001).
9. Breiter, H.C., Aharon, I., Kahneman, D., Dale, A. & Shizgal, P. Functional imaging of neural responses to expectancy and experience of monetary gains and losses. *Neuron* **30**, 619–639 (2001).
10. O'Doherty, J.P., Deichmann, R., Critchley, H.D. & Dolan, R.J. Neural responses during anticipation of a primary taste reward. *Neuron* **33**, 815–826 (2002).
11. O'Doherty, J.P., Dayan, P., Friston, K., Critchley, H. & Dolan, R.J. Temporal difference models and reward-related learning in the human brain. *Neuron* **38**, 329–337 (2003).
12. Sutton, R.S. & Barto, A.G. *Reinforcement Learning* (MIT Press, Cambridge, Massachusetts, 1998).
13. Houk, J.C., Adams, J.L. & Barto, A.G. in *Models of Information Processing in the Basal Ganglia* (eds. Houk, J.C., Davis, J.L. & Beiser, D.G.) 249–270 (MIT Press, Cambridge, Massachusetts, 1995).
14. Schultz, W., Dayan, P. & Montague, P.R. A neural substrate of prediction and reward. *Science* **275**, 1593–1599 (1997).
15. Doya, K. Complementary roles of basal ganglia and cerebellum in learning and motor control. *Curr. Opin. Neurobiol.* **10**, 732–739 (2000).
16. McClure, S.M., Berns, G.S. & Montague, P.R. Temporal prediction errors in a passive learning task activate human striatum. *Neuron* **38**, 339–346 (2003).
17. Mesulam, M.M. & Mufson, E.J. Insula of the old world monkey. III: Efferent cortical output and comments on function. *J. Comp. Neurol.* **212**, 38–52 (1982).
18. Cavada, C., Company, T., Tejedor, J., Cruz-Rizzolo, R.J. & Reinoso-Suarez, F. The anatomical connections of the macaque monkey orbitofrontal cortex. *Cereb. Cortex* **10**, 220–242 (2000).
19. Chikama, M., McFarland, N.R., Amaral, D.G. & Haber, S.N. Insular cortical projections to functional regions of the striatum correlate with cortical cytoarchitectonic organization in the primate. *J. Neurosci.* **17**, 9686–9705 (1997).
20. Balleine, B.W. & Dickinson, A. The effect of lesions of the insular cortex on instrumental conditioning: evidence for a role in incentive memory. *J. Neurosci.* **20**, 8954–8964 (2000).
21. Knutson, B., Fong, G.W., Bennett, S.M., Adams, C.M. & Hommer, D. A region of mesial prefrontal cortex tracks monetarily rewarding outcomes: characterization with rapid event-related fMRI. *Neuroimage* **18**, 263–272 (2003).
22. Ullsperger, M. & von Cramon, D.Y. Error monitoring using external feedback: specific roles of the habenular complex, the reward system, and the cingulate motor area revealed by functional magnetic resonance imaging. *J. Neurosci.* **23**, 4308–4314 (2003).
23. O'Doherty, J., Critchley, H., Deichmann, R. & Dolan, R.J. Dissociating valence of outcome from behavioral control in human orbital and ventral prefrontal cortices. *J. Neurosci.* **23**, 7931–7939 (2003).
24. Koepp, M.J. *et al.* Evidence for striatal dopamine release during a video game. *Nature* **393**, 266–268 (1998).
25. Elliott, R., Friston, K.J. & Dolan, R.J. Dissociable neural responses in human reward systems. *J. Neurosci.* **20**, 6159–6165 (2000).
26. Knutson, B., Adams, C.M., Fong, G.W. & Hommer, D. Anticipation of increasing monetary reward selectively recruits nucleus accumbens. *J. Neurosci.* **21**, RC159 (2001).
27. Pagnoni, G., Zink, C.F., Montague, P.R. & Berns, G.S. Activity in human ventral striatum locked to errors of reward prediction. *Nat. Neurosci.* **5**, 97–98 (2002).
28. Elliott, R., Newman, J.L., Longe, O.A. & Deakin, J.F. Differential response patterns in the striatum and orbitofrontal cortex to financial reward in humans: a parametric functional magnetic resonance imaging study. *J. Neurosci.* **23**, 303–307 (2003).
29. Haruno, M. *et al.* A neural correlate of reward-based behavioral learning in caudate nucleus: a functional magnetic resonance imaging study of a stochastic decision task. *J. Neurosci.* **24**, 1660–1665 (2004).
30. Reynolds, J.N. & Wickens, J.R. Dopamine-dependent plasticity of corticostriatal synapses. *Neural Net.* **15**, 507–521 (2002).
31. Tremblay, L. & Schultz, W. Reward-related neuronal activity during go-nogo task performance in primate orbitofrontal cortex. *J. Neurophysiol.* **83**, 1864–1876 (2000).
32. Critchley, H.D., Mathias, C.J. & Dolan, R.J. Neural activity in the human brain relating to uncertainty and arousal during anticipation. *Neuron* **29**, 537–545 (2001).
33. Rogers, R.D. *et al.* Choosing between small, likely rewards and large, unlikely rewards activates inferior and orbital prefrontal cortex. *J. Neurosci.* **19**, 9029–9038 (1999).
34. Rolls, E.T. The orbitofrontal cortex and reward. *Cereb. Cortex* **10**, 284–294 (2000).
35. Hanakawa, T. *et al.* The role of rostral Brodmann area 6 in mental-operation tasks: an integrative neuroimaging approach. *Cereb. Cortex* **12**, 1157–1170 (2002).
36. Owen, A.M., Doyon, J., Petrides, M. & Evans, A.C. Planning and spatial working memory: a positron emission tomography study in humans. *Eur. J. Neurosci.* **8**, 353–364 (1996).
37. Baker, S.C. *et al.* Neural systems engaged by planning: a PET study of the Tower of London task. *Neuropsychologia* **34**, 515–526 (1996).
38. Middleton, F.A. & Strick, P.L. Basal ganglia and cerebellar loops: motor and cognitive circuits. *Brain Res. Brain Res. Rev.* **31**, 236–250 (2000).
39. Haber, S.N., Kunishio, K., Mizobuchi, M. & Lynd-Balta, E. The orbital and medial prefrontal circuit through the primate basal ganglia. *J. Neurosci.* **15**, 4851–4867 (1995).
40. Eagle, D.M., Humby, T., Dunnett, S.B. & Robbins, T.W. Effects of regional striatal lesions on motor, motivational, and executive aspects of progressive-ratio performance in rats. *Behav. Neurosci.* **113**, 718–731 (1999).
41. Pears, A., Parkinson, J.A., Hopewell, L., Everitt, B.J. & Roberts, A.C. Lesions of the orbitofrontal but not medial prefrontal cortex disrupt conditioned reinforcement in primates. *J. Neurosci.* **23**, 11189–11201 (2003).
42. Hikosaka, O. *et al.* Parallel neural networks for learning sequential procedures. *Trends Neurosci.* **22**, 464–471 (1999).
43. Mijnster, M.J. *et al.* Regional and cellular distribution of serotonin 5-hydroxytryptamine2a receptor mRNA in the nucleus accumbens, olfactory tubercle, and caudate putamen of the rat. *J. Comp. Neurol.* **389**, 1–11 (1997).
44. Compan, V., Segu, L., Buhot, M.C. & Daszuta, A. Selective increases in serotonin 5-HT1B/1D and 5-HT2A/2C binding sites in adult rat basal ganglia following lesions of serotonergic neurons. *Brain Res.* **793**, 103–111 (1998).
45. Celada, P., Puig, M.V., Casanovas, J.M., Guillazo, G. & Artigas, F. Control of dorsal raphe serotonergic neurons by the medial prefrontal cortex: involvement of serotonin-1A, GABA(A), and glutamate receptors. *J. Neurosci.* **21**, 9917–9929 (2001).
46. Martin-Ruiz, R. *et al.* Control of serotonergic function in medial prefrontal cortex by serotonin-2A receptors through a glutamate-dependent mechanism. *J. Neurosci.* **21**, 9856–9866 (2001).
47. Hikosaka, K. & Watanabe, M. Delay activity of orbital and lateral prefrontal neurons of the monkey varying with different rewards. *Cereb. Cortex* **10**, 263–271 (2000).
48. Shidara, M. & Richmond, B.J. Anterior cingulate: single neuronal signals related to degree of reward expectancy. *Science* **296**, 1709–1711 (2002).
49. Matsumoto, K., Suzuki, W. & Tanaka, K. Neuronal correlates of goal-based motor selection in the prefrontal cortex. *Science* **301**, 229–232 (2003).